

1 **Title: Evolution of olfactory receptors tuned to mustard oils in herbivorous Drosophilidae**

2

3 **Authors:** #Teruyuki Matsunaga^{1*}, #Carolina E. Reisenman², #Benjamin Goldman-Huertas³, Philipp
4 Brand⁴, Kevin Miao¹, Hiromu C. Suzuki¹, Kirsten I. Verster¹, Santiago R. Ramírez⁴, Noah K.
5 Whiteman^{1*}

6 #Equal contributions

7 **Affiliations:**

8 ¹ Department of Integrative Biology, University of California Berkeley, Berkeley, CA

9 ² Department of Molecular and Cell Biology, University of California Berkeley, Berkeley, CA

10 ³ Department of Molecular and Cellular Biology, University of Arizona, Tucson, AZ

11 ⁴ Department of Evolution and Ecology, University of California Davis, Davis, CA

12 *Correspondence to: whiteman@berkeley.edu (N.K.W.) and teru.matsu0208@berkeley.edu (T.M.)

13

14 **Keywords:**

15 *Drosophila melanogaster*, *Scaptomyza flava*, herbivory, evolution, olfaction, isothiocyanate,

16 chemoreceptor, SSR, olfactory receptor, wasabi, Brassicaceae, Or67b, gene duplication,

17 neofunctionalization, subfunctionalization, specialization, olfactory specialization

18

19

20

21

22

23

24 **ABSTRACT:**

25 The diversity of herbivorous insects is attributed to their propensity to specialize on toxic plants. In an
26 evolutionary twist, toxins betray the identity of their bearers when herbivores co-opt them as cues for
27 host-plant finding, but the mechanisms underlying this process are poorly understood. We focused on
28 *Scaptomyza flava*, an herbivorous drosophilid specialized on isothiocyanate (ITC)-producing
29 (Brassicaceae) plants, and identified *Or67b* paralogs that were triplicated as mustard-specific herbivory
30 evolved. Using heterologous systems for the expression of olfactory receptors, we found that *S. flava*
31 *Or67b*s, but not homologs from microbe-feeding relatives, responded selectively to ITCs, each paralog
32 detecting different ITC subsets. Consistent with this, *S. flava* was attracted to ITCs, as was *Drosophila*
33 *melanogaster* expressing *S. flava Or67b3* in the homologous *Or67b* olfactory circuit. Thus, our results
34 show that plant toxins were likely co-opted as olfactory attractants through gene duplication and
35 functional specialization (neofunctionalization and subfunctionalization) in drosophilid flies.

36

37

38

39

40

41

42

43

44

45

46 INTRODUCTION

47 Many plant molecules used in food, agriculture and medicine first evolved as defenses against
48 natural enemies ¹. Among the most familiar are reactive electrophiles that produce pain when eaten,
49 including diallyl disulfide and thiosulfinates in Alliaceae (*e.g.*, garlic), α , β -unsaturated aldehydes in
50 Lauraceae (*e.g.*, cinnamon), and isothiocyanates (ITCs) in Brassicaceae (*e.g.*, arugula, radish, and
51 wasabi). These electrophiles activate the ‘wasabi taste receptor’ TrpA1, which is conserved in flies and
52 humans ². Although ITCs are potent natural insecticides aversive to most insects, including *D.*
53 *melanogaster* ³, some insect species are specialized on ITC-bearing Brassicaceae (mustards). This
54 insect-plant interaction has been important in advancing the field of co-evolution ⁴. Brassicaceae
55 specialists from many insect orders (*e.g.*, Diptera ⁵, Heteroptera ⁶, Hemiptera ⁷, and Lepidoptera ⁸) can
56 be trapped with ITC baits in crop fields, revealing an evolutionary twist of fate in which mustard
57 specialist insects use ancestrally aversive electrophiles as olfactory cues for host-plant finding ⁹.
58 However, the evolutionary mechanisms underlying the chemosensory adaptations of insect herbivores to
59 defensive plant compounds are widely unknown ¹⁰. Identifying these mechanisms can help us
60 understand the evolution of herbivorous insect species, 90% of which are specialized on a limited set of
61 host plants ¹¹.

62 *Scaptomyza* represents a compelling genus to investigate how specialist herbivores evolved to
63 co-opt plant defenses as host finding cues. Phylogenetically nested within *Drosophila*, *Scaptomyza* is the
64 sister group to the Hawaiian *Drosophila* radiation ¹², and contains many herbivorous species with
65 varying degrees of specialization on Brassicaceae and Caryophyllaceae ¹³. Adult females make feeding
66 punctures in living leaves using sclerotized and dentate ovipositors ¹⁴, and their larvae hatch directly into
67 the mesophyll tissue, which they mine ¹⁵, an unusual life history within the Drosophilidae. *S. flava*
68 specializes on Brassicaceae ¹⁶ and, like humans and *D. melanogaster*, uses the mercapturic pathway to
69 detoxify ITCs ¹⁷. *S. flava* was first reported from *Arabidopsis thaliana* in North America as *S. flaveola*

70 ¹⁸. Thus, genomic and genetic tools of both *Arabidopsis* and *Drosophila* can be utilized to dissect both
71 sides of the plant-herbivore equation. Herbivory evolved ca. 10-15 million years ago in *Scaptomyza*
72 (Figure 1A) and so it provides an unusually useful context to understand the evolutionary and functional
73 mechanisms underlying chemosensory specialization, because the major herbivorous insect radiations
74 (e.g. Lepidoptera¹⁹, Phytophaga²⁰) are much more ancient in origin.

75 *S. flava* lost three olfactory receptor (*Or*) genes encoding canonical yeast-associated receptors
76 after divergence from microbe-feeding drosophilid relatives, contemporaneous with the evolution of
77 herbivory²¹. However, the loss of function does not explain how herbivorous *Scaptomyza* species
78 evolved attraction to Brassicaceae plants (a gain of function phenotype).

79 Gain of function through gene duplication and subsequent divergence plays an important role in
80 evolutionary innovation and is often associated with trophic transitions²². Gene and whole genome
81 duplications in Brassicaceae in the last 90 million years resulted in the evolution of glucosinolates, the
82 precursors of ITC compounds²³. Reciprocally, in diverse Brassicaceae-specialist pierid butterflies,
83 enzymes that divert hydrolysis of aliphatic glucosinolates away from ITC production to less toxic
84 nitriles evolved in tandem, underpinning their diversification and highlighting the importance of gene
85 family evolution in this co-evolutionary arms race²⁴. While our understanding of detoxification in plant-
86 herbivore systems has grown rapidly over the past decade²⁵, the evolutionary mechanisms underlying
87 the chemosensory basis of hostplant orientation and finding remain relatively unknown. Here we
88 investigated the extent to which duplication of chemosensory genes in the *S. flava* lineage contributed to
89 attraction to specific host-plant volatiles, including ITCs.

90 We took a genes-first approach to study olfactory host-plant specialization in *S. flava*. Three
91 chemoreceptor protein families (olfactory receptors -Ors-, ionotropic receptors -Irs-, and nociceptive
92 receptors -Trps-) are candidates for mediating responses to host-specific volatile electrophiles such as

93 ITCs²⁶. In particular, insect Ors are collectively sensitive to a variety of odorants important for food and
94 host finding, avoidance of predators, and animal communication, including aversive chemicals²⁷,
95 pheromones²⁸⁻³⁰, and host-, oviposition-, and food-related attractive compounds³¹⁻³³. Accordingly, we
96 scanned the genome sequence of *S. flava* to identify rapidly evolving Ors and found a lineage-specific
97 gene copy number expansion of the olfactory receptor gene *Or67b* that we named *Or67b1*, *Or67b2*, and
98 *Or67b3*. The coding sequences of these three paralogs exhibit signatures of positive natural selection
99 and duplicated likely within the last ca. 15 million years, at the base of the mustard-feeding clade. In
100 contrast, *Or67b* is present as a single copy under strong evolutionary constraint across the Drosophilidae
101 ^{21,34-35}, including two focal species included here, the microbe-feeding close relative *S. pallida*
102 (subgenus *Parascaptomyza*), and the more distantly related *D. melanogaster*. Our *in vivo* functional
103 characterizations of all full-length Or67b proteins from these three species show that the three *S. flava*
104 Or67b proteins, but not the conserved Or67b proteins from its microbe-feeding relatives, responded
105 selectively and sensitively to volatile ITCs. Concomitantly, we found a population of *S. flava* antennal
106 olfactory sensory neurons (OSNs) responsive to ITCs. In agreement with these results, *S. flava*, but not
107 *S. pallida* or *D. melanogaster*, is attracted to odors from Brassicaceae plants, including single ITC
108 compounds. Expression of *Sfla* Or67b3 in the *D. melanogaster* homologous Or67b olfactory circuit
109 indicates that *Sfla* Or67b3 can confer odor-oriented responses towards ITCs. Finally, our genetic
110 silencing experiments demonstrate that the Or67b olfactory circuit mediates attraction in *D.*
111 *melanogaster*. These findings support the hypothesis that simple evolutionary changes in the odorant
112 tuning of an Or may be sufficient for changing the identity of the odorants that evoke behavioral
113 responses^{28,36-38}. Of particular ecological significance is that the three *Sfla* Or67b proteins shifted the
114 odor-receptive ranges from the typical ancestral Or67 drosophilid response profile of ketones, alcohols,
115 and aldehydes³⁹⁻⁴⁰ to ITCs, an entirely different chemical class of compounds. In summary, our results

116 suggest a relatively simple sensory mechanism by which mustard-specialist herbivorous insects may
117 have evolved olfactory attraction towards host-plant ITCs, via gene duplication followed by
118 neofunctionalization (see discussion) of a specific clade of otherwise highly conserved Ors in the
119 Drosophilidae.

120

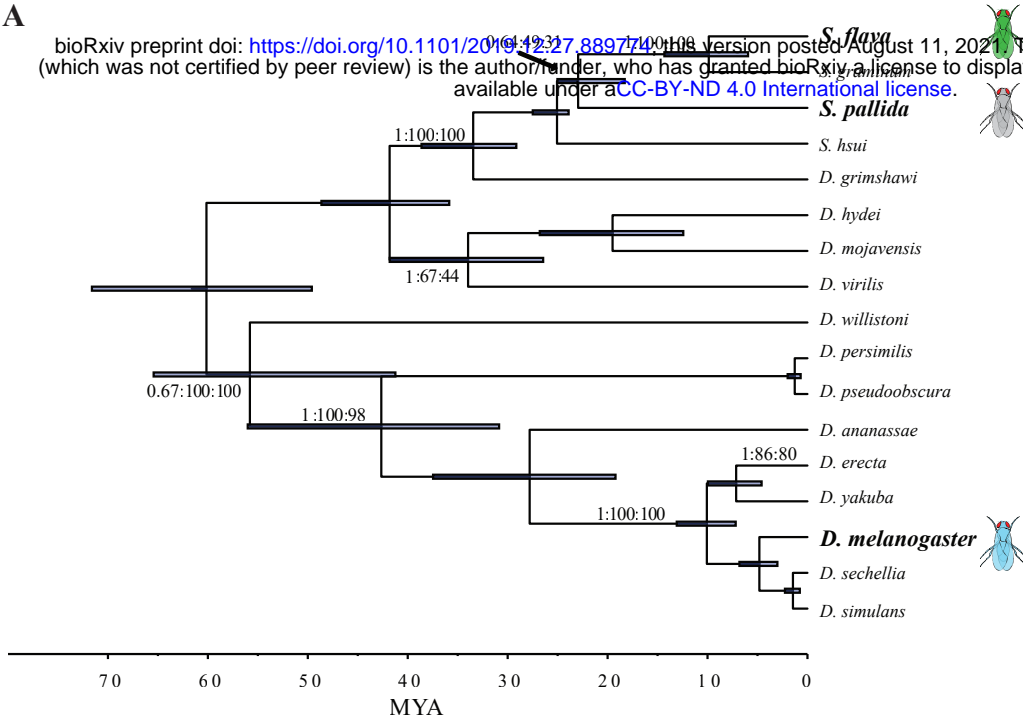
121 RESULTS

122 **Phylogenetic analysis identified *Or67b* paralogs as candidates mediating the detection of** 123 **ecologically relevant host-plant odorants**

124 To search for candidate ITC-detecting chemosensory receptors in *S. flava*, we conducted a
125 phylogenetic analysis of the Or protein sequences of *S. flava* and four other *Drosophila* species to
126 identify *Scaptomyza*-specific gene losses and gains (Figure supplement 1) as well as those that were
127 rapidly evolving at the protein level, regardless of duplication history. The Or topology was largely
128 congruent with previous *Drosophila* Or gene trees²¹, except for some deeper nodes, which had low
129 bootstrap support. In addition to a previous analysis of Or coding sequences using a branch-site test to
130 identify *Scaptomyza* Or codons likely evolving under positive selection²¹, we also fit simpler
131 foreground/background branch models, as implemented in PAML, to scan for Ors whose sequences
132 were evolving under divergent selection regimes from the *Drosophila* background.⁴¹ Out of seventy-five
133 *S. flava* branches tested, seven branch models, corresponding to paralogs of *Or63a*, *Or67b* and *Or98a* in
134 *D. melanogaster*, inferred a foreground rate larger than one, consistent with a high rate of fixation of
135 nonsynonymous mutation during positive selection across the Or coding sequence (supplementary file
136 1). Among these receptors, *Or63a* is only expressed in *D. melanogaster* larvae⁴², and the *Or98a*-like
137 genes found in *Scaptomyza* have no *D. melanogaster* homologs and have not been characterized
138 functionally. In contrast, *Or67b* modulates oviposition behavior in adult *D. melanogaster*⁴³, and is

A

bioRxiv preprint doi: <https://doi.org/10.1101/2019.12.27.889774>; this version posted August 11, 2021. The copyright holder for this preprint (which was not certified by peer review) is the author/funder, who has granted bioRxiv a license to display the preprint in perpetuity. It is made available under aCC-BY-ND 4.0 International license.



B

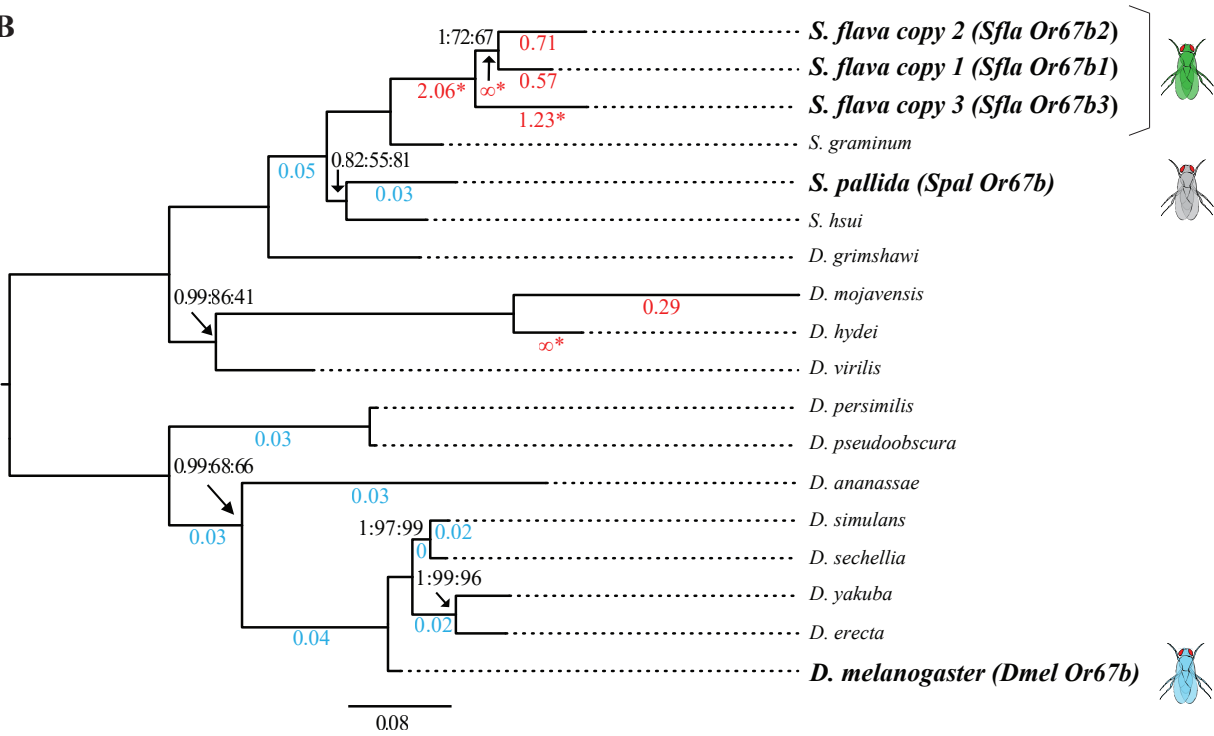


Figure 1 Maximum likelihood (ML) phylogeny of *Or67b* in Drosophilidae.

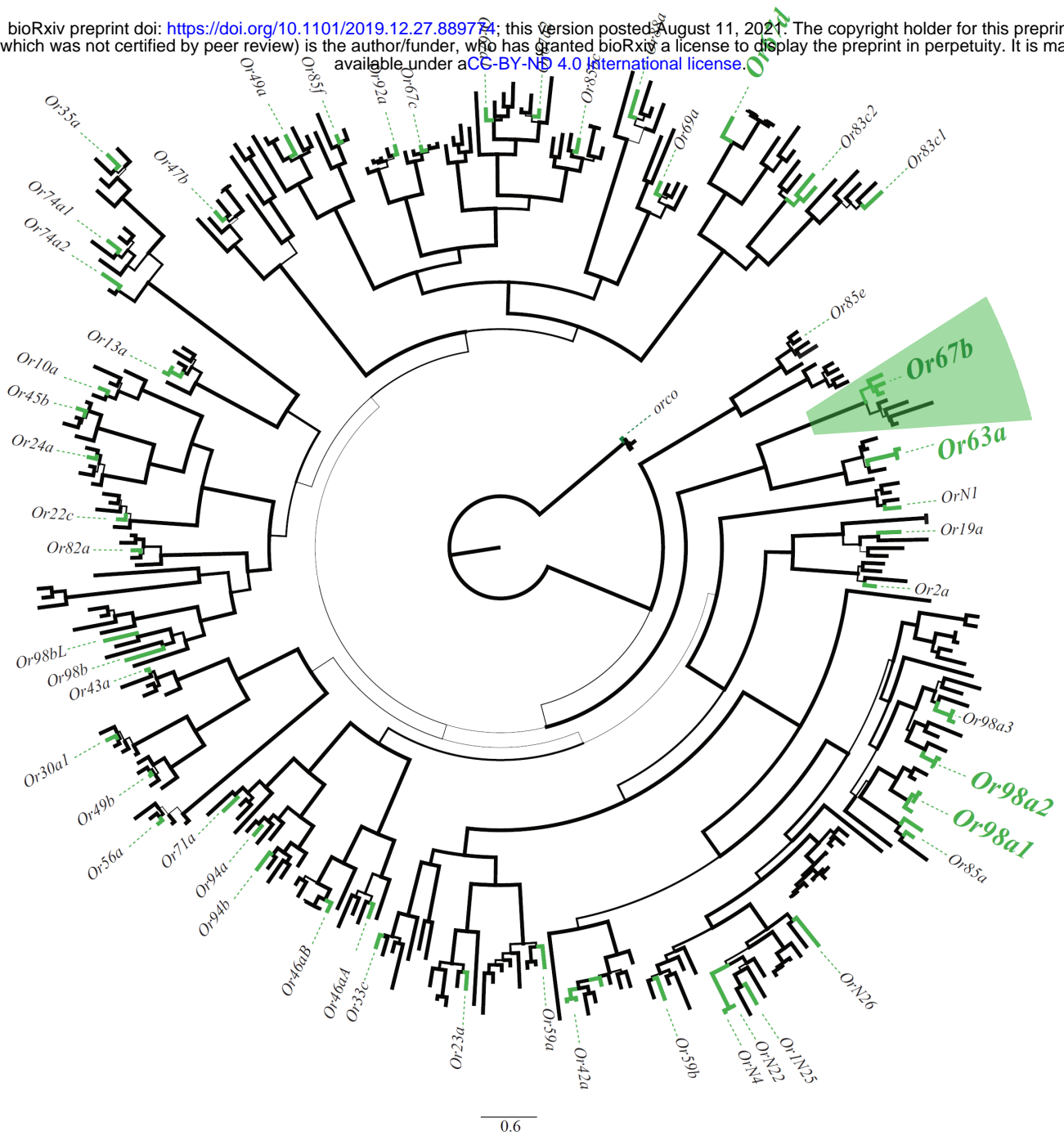
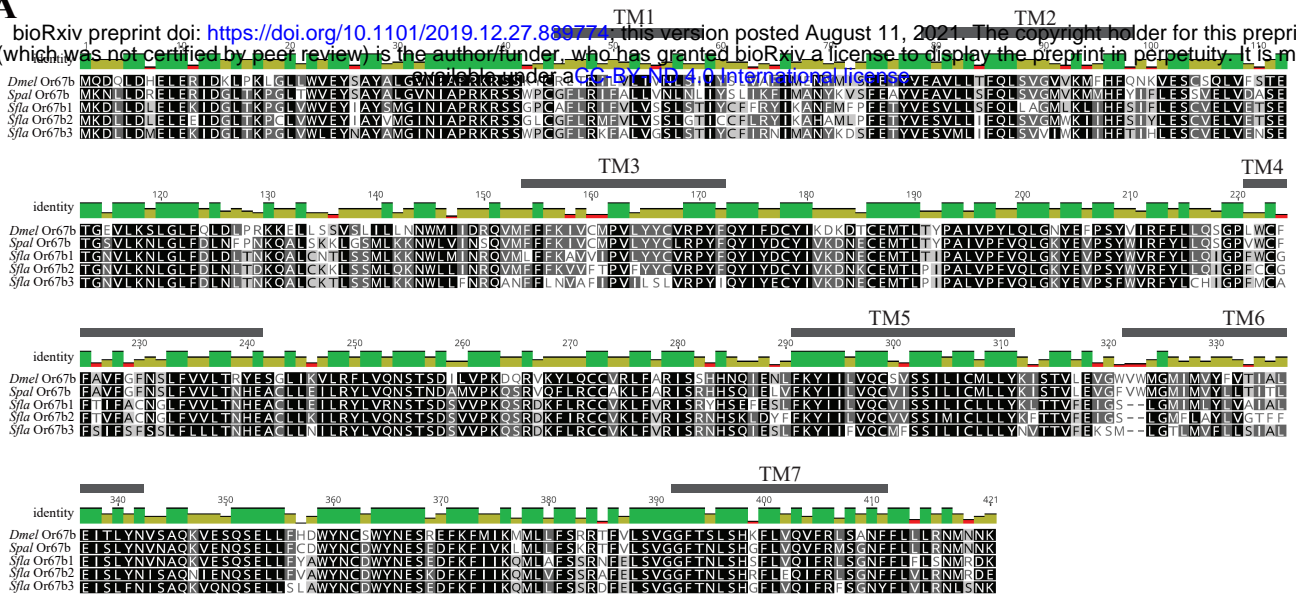


Figure supplement 1 Maximum likelihood (ML) phylogeny of *Ors* in Drosophilidae.

A bioRxiv preprint doi: <https://doi.org/10.1101/2019.12.27.889774>; this version posted August 11, 2021. The copyright holder for this preprint (which was not certified by peer review) is the author/funder, who has granted bioRxiv a license to display the preprint in perpetuity. It is made available under aCC-BY-NC 4.0 International license.



B

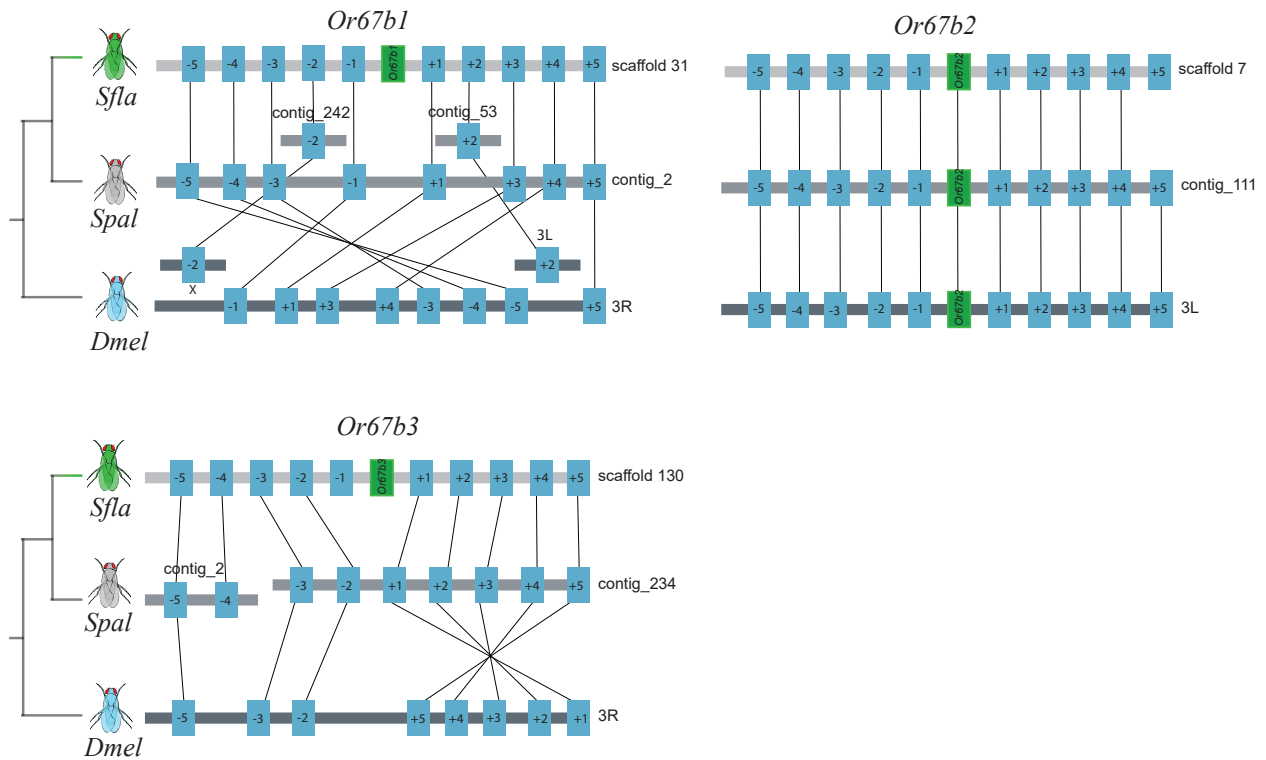


Figure supplement 2 Or67b protein alignment and micro-synteny patterns of scaffolds from *S. flava*, *S. pallida*, and *D. melanogaster*.

139 implicated in selection of oviposition sites in *D. mojavensis*⁴⁴, making it a good candidate for the
140 olfactory adaptation of *Scaptomyza* to a novel host niche. After expanding the representation of *Or67b*
141 orthologs in a phylogenetic analysis and conducting branch tests in PAML on all single branches on the
142 *Or67b* phylogeny, we found significantly elevated d_N/d_S exclusively in *S. flava* and *D. mojavensis*
143 *Or67b* (Figure 1B and Supplementary file 1). Furthermore, synteny analysis confirmed that the regions
144 upstream and downstream of the two non-syntenic *Or67b* copies in *S. flava* are present in both *S. pallida*
145 and *D. melanogaster*. Thus, the absence of each paralog in *S. pallida* and *D. melanogaster* is not a
146 genome assembly artefact but rather, an actual absence (Figure supplement 2A, B).

147

148 ***S. flava* Or67bs respond specifically to mustard plant odors**

149 Because *Or67b* is triplicated exclusively in the *S. flava* lineage and likely evolved under positive
150 selection since its divergence from copies in non-herbivorous species, we next investigated whether *Sfla*
151 Or67bs acquired novel ligand-binding sensitivity towards odorants characteristic for the mustard hosts
152 of *S. flava* (Figure 1). First, we confirmed that all three *S. flava* paralogs and the *S. pallida* ortholog are
153 expressed in adults (Source data). To study the odor-response profile of Or67b across species, we then
154 heterologously expressed the Or67b paralogs in the *D. melanogaster* olfactory at1 or ab3A neurons
155 lacking endogenous Ors^{28,45}, and measured electrophysiological responses to an array of mustard
156 secondary plant compounds and other odors (Figure 2A and Figure supplement 3A). Ab3A neurons
157 expressing *Sfla* Or67b1, *Sfla* Or67b3, *Spal* Or67b, and *Dmel* Or67b showed spontaneous bursts of action
158 potentials (as described for other Ors expressed in these neurons⁴⁶), whereas neurons expressing *Sfla*
159 Or67b2 showed spontaneous activity only when expressed in at1 OSNs. Thus, we used the “at1 empty
160 neuron” system for studying the olfactory responses of *Sfla* Or67b2, and the “ab3A empty neuron”
161 system for investigating the responses of all other Or67b proteins.

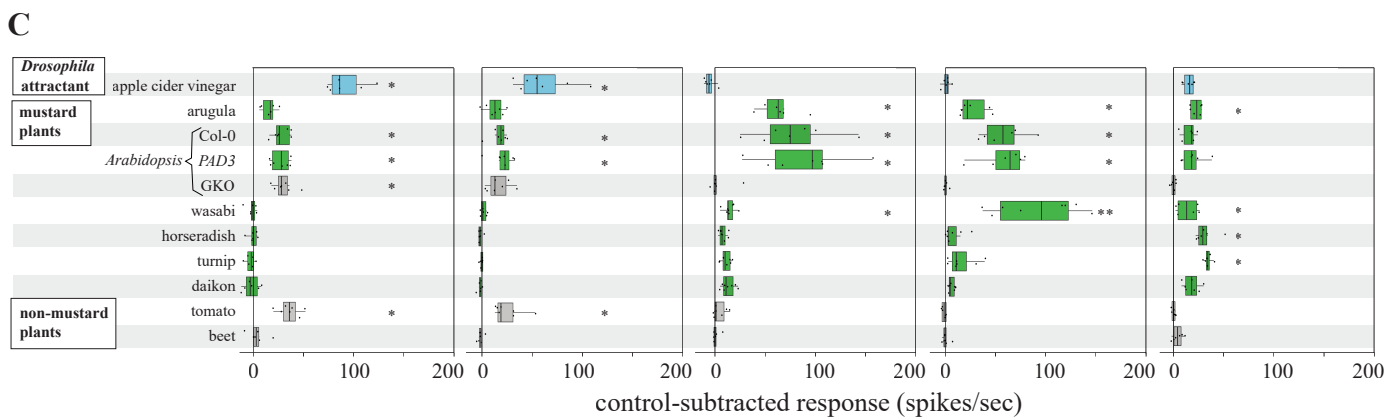
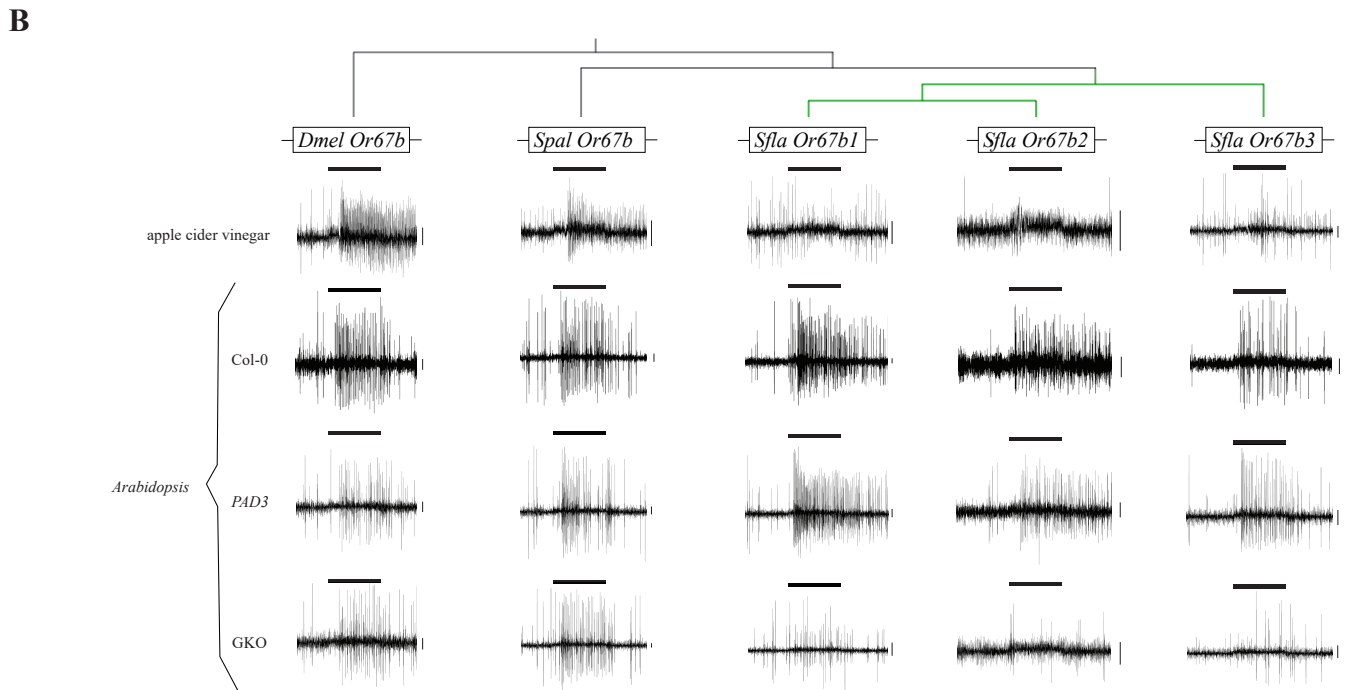
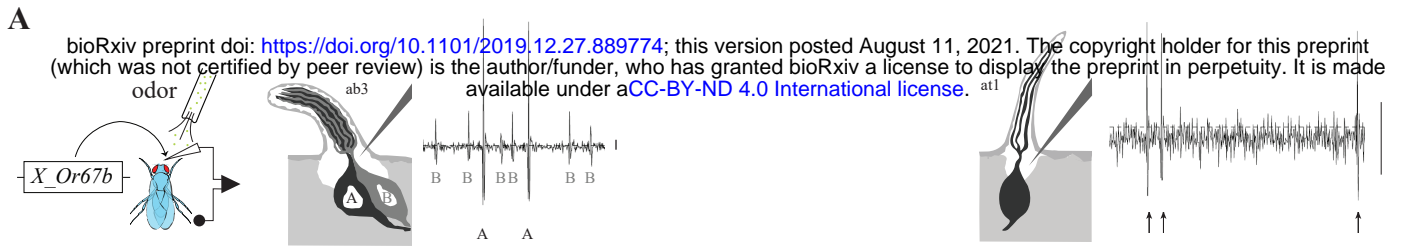


Figure 2 Responses of homologs Or67bs from *D. melanogaster*, *S. pallida*, and *S. flava* expressed in the *D. melanogaster* empty neuron systems to stimulation with natural odor blends.

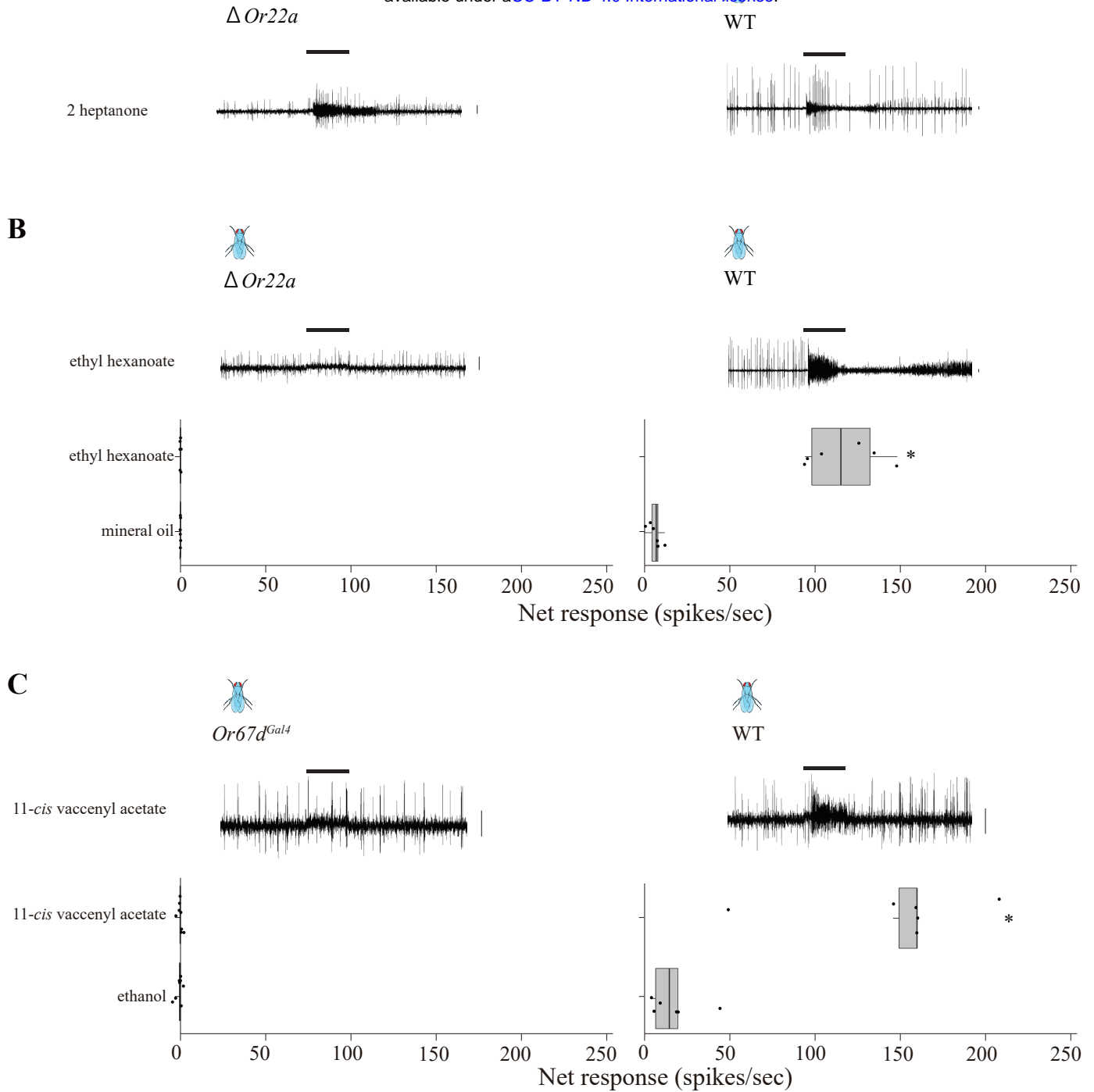


Figure supplement 3 Or22a and Or67b are not expressed in the ab3A and the at1 empty neuron systems.

162 In order to test which odors specifically activate *Sfla* Or67b paralogs, we tested the responses of
163 all Or67bs to stimulation with apple cider vinegar (a potent *D. melanogaster* attractant⁴⁷), crushed
164 arugula leaves (*Eruca vesicaria*, a mustard), and crushed tomato leaves (*Solanum lycopersicum*, a non-
165 mustard plant that releases large quantities of volatile organic compounds⁴⁸). OSNs expressing *Dmel*
166 Or67b and *Spal* Or67b, but not those expressing any of the *Sfla* Or67 paralogs, responded strongly to
167 stimulation with apple cider vinegar (Figure 2B, C), indicating that the *Sfla* Or67b paralogs lost the
168 ancestral odorant sensitivity. Volatiles from crushed tomato leaves activated both *Dmel* Or67b and *Spal*
169 Or67b. In contrast, all *Sfla* Or67b paralogs responded to volatiles from crushed arugula leaves, but not to
170 those from tomato (Figure 2C), suggesting that *Sfla* Or67bs specifically respond to volatiles
171 characteristic of their hosts but not to those from non-hosts.

172 In contrast to tomato plants, Brassicaceae plants, including arugula, produce glucosinolates,
173 some of which are hydrolyzed into ITCs upon tissue damage⁴⁹. To test if responses of *Sfla* Or67bs to
174 mustard leaf odors are mediated by ITCs and/or by other mustard volatile plant compounds, we used
175 crushed leaves of wild-type *A. thaliana* (Col-0) and two loss of function mutants generated in the Col-0
176 background. One of these mutants (GKO) is deficient in the production of ITC-precursors derived from
177 aliphatic and indolic glucosinolates as well as camalexin⁵⁰⁻⁵¹ and does not release ITCs upon wounding
178^{50,52-54}, whereas the control line (PAD3) produces these glucosinolates but not camalexin^{51,54}.
179 Stimulation with both wild-type *A. thaliana* and *PAD3* mutant leaves, which can produce ITCs,
180 activated OSNs expressing *Sfla* Or67b1, b2 and b3, whereas stimulation with GKO mutant leaves did
181 not ($p > 0.05$ in all cases; Figure 2C). This suggests that ITCs, but not other leaf volatiles, activate the
182 three *Sfla* paralogs. In contrast, *Dmel* Or67b expressing OSNs showed similar responses to all three *A.*
183 *thaliana* genotypes (Figure 2C), in agreement with the reported responses of this Or to green leaf
184 volatiles (GLVs)⁵⁵. Similar to *Dmel* Or67b, OSNs expressing *Spal* Or67 responded to all *A. thaliana*

185 genotypes, but with low spike frequency (Figure 2C). Because GKO plants differed from both *PAD3*
186 and Col-0 plants only in the capability of producing ITCs⁵⁰⁻⁵¹, these results demonstrate that the *Sfla*
187 Or67b paralogs are selectively activated by these signature chemical compounds of Brassicaceae. In
188 contrast, *Dmel* and *Spal* Or67b were activated by non-ITC mustard and non-mustard plant volatiles,
189 consistent with previous studies⁵⁶⁻⁵⁷.

190 Because mustard plant roots release a variety of volatile organic compounds (VOCs) including
191 ITCs, but not GLVs⁵⁸⁻⁶⁰, we also used preparations of these tissues as stimuli. We prepared root
192 homogenates of four mustard plant species, including wasabi (*Eutrema japonicum*)⁵⁸, horseradish
193 (*Armoracia rusticana*)⁵⁸, turnip (*Brassica rapa*)⁵⁹, daikon (*Raphanus sativus*)⁶⁰, and a non-mustard
194 control root vegetable species (beet, *Beta vulgaris*)⁶¹ from a different plant order. Interestingly, OSNs
195 expressing each *Sfla* Or67b paralog differed in responsiveness to mustard plant leaf and root volatiles.
196 For example, stimulation with arugula elicited strongest responses in neurons expressing *Sfla* Or67b1
197 (64 net spikes/sec; median; Figure 2C), stimulation with wasabi root odors produced strongest responses
198 in neurons expressing *Sfla* Or67b2 (96 net spikes/sec), and stimulation with turnip roots produced the
199 strongest responses in OSNs expressing *Sfla* Or67b3 (34 net spikes/sec).

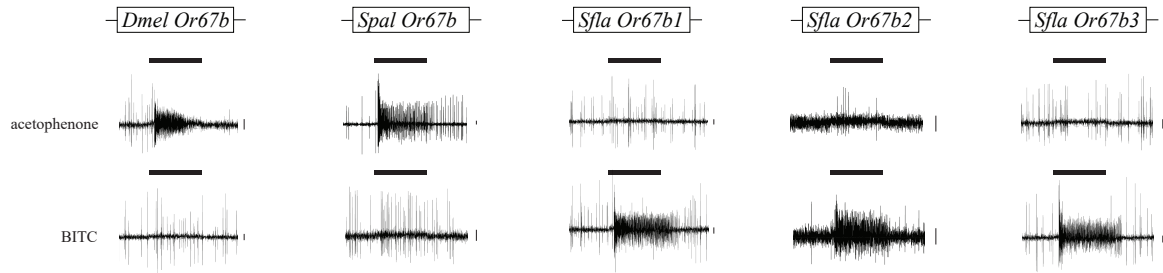
200

201 ***S. flava* Or67b paralogs have different ITC selectivity**

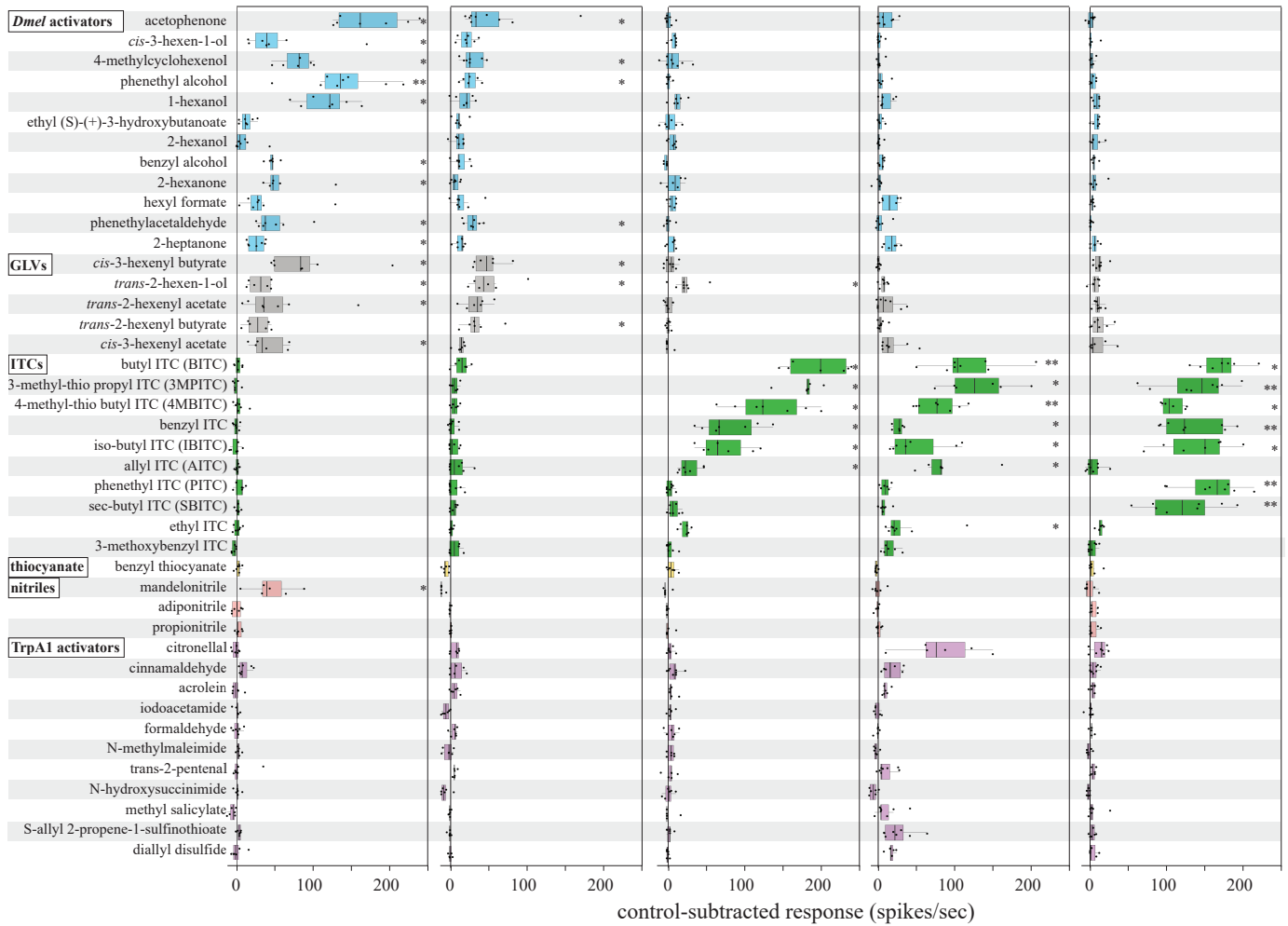
202 We next investigated the odor-tuning profiles of Or67b copies from all tested species by testing
203 their responses to a panel of 42 individual odorants (all tested at 1:100 vol/vol), which included ITCs,
204 nitriles, GLVs, and odorants known to activate *Dmel* Or67b, including ketones, esters, and alcohols⁵⁵;
205 Figure 3B). Testing this broad array of odors from diverse chemical classes allowed us to cover a wide
206 range of known secondary plant compounds and other appetitive odors to investigate the odor-response
207 profiles of Or67b proteins across species^{10, 62}.

A

bioRxiv preprint doi: <https://doi.org/10.1101/2019.12.27.889774>; this version posted August 11, 2021. The copyright holder for this preprint (which was not certified by peer review) is the author/funder, who has granted bioRxiv a license to display the preprint in perpetuity. It is made available under aCC-BY-ND 4.0 International license.



B



C

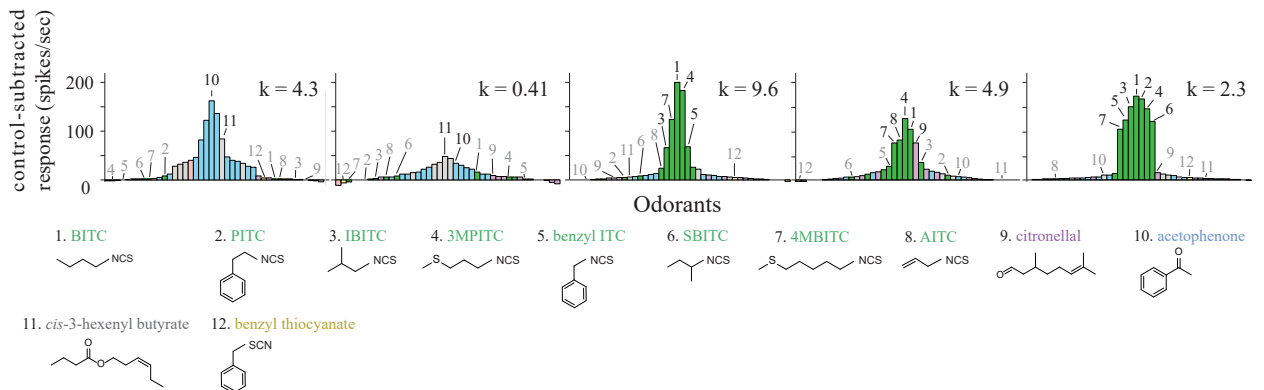


Figure 3 Responses of homologs Or67bs from *D. melanogaster*, *S. pallida* and *S. flava* expressed in the *D. melanogaster* empty neuron systems to stimulation with single odorants.

208 We first verified the known *Dmel* Or67b response profile ⁵⁵, which includes many chemicals
209 from a diverse number of chemical classes: 13/17 odorants categorized as *Dmel* activators and GLVs
210 evoked responses (one-sample signed rank tests, $p < 0.05$; Figure 3). *Spal* Or67b responded to a smaller
211 number of odorants within those categories (7/17 odorants; $p < 0.05$). Strikingly, only one of the
212 compounds that elicited responses from *Dmel* Or67b and *Spal* Or67b (*trans*-2-hexen-1-ol) evoked
213 responses from *Sfla* Or67b1 (median=22 net spikes/second; $p < 0.05$), but none of the 17 odorants
214 categorized as *Dmel* activators and GLVs evoked responses from *Sfla* Or67b2 or *Sfla* Or67b3 (Figure
215 3B; $p > 0.05$ in all cases). While various ITCs evoked responses from each of the *S. flava* paralogs (7/10
216 ITCs for all three paralogs; $p < 0.05$), none evoked responses from *Dmel* Or67b or *Spal* Or67b ($p > 0.05$;
217 Figure 3A, B). Tuning curves (Figure 3C) of all Or67b proteins show that *Sfla* Or67bs have response
218 profiles distinct from those of *Dmel* Or67b and *Spal* Or67b, whereas non-ITC compounds evoke the
219 strongest responses (acetophenone and *cis*-3-hexenyl-butyrate, respectively, center of the distribution,
220 yellow bars; Figure 3C). All *Sfla* Or67b paralogs had strongest responses to ITC compounds (center of
221 the distribution, green bars; Figure 3C). *Sfla* Or67b1 had the narrowest odorant-receptive range,
222 responding to a smaller subset of ITC compounds tested, indicated by the high kurtosis and sharp peak
223 of the tuning curve. Overall, these results demonstrate that *Dmel* Or67b and *Spal* Or67b do not respond
224 to ITCs and have similar odor-response profiles, while each *Sfla* Or67b paralog is differentially
225 responsive to ITCs that are found in diverse mustard species ⁴⁹.

226 We then tested whether *Sfla* Or67b paralogs differed in their ITC selectivity, possibly allowing
227 flies to differentiate between different mustard plant species. We stimulated OSNs expressing *Sfla*
228 paralogs with serial dilutions of eight selected ITCs that evoked the strongest responses at 1:100 vol/vol
229 (Figure 3B). Because the magnitude of the responses may be reduced when an Or is expressed in at 1
230 OSNs (in comparison with responses when expressed in ab3A OSNs ⁶³) we included both non-

231 normalized and normalized median responses for all Or-odorant pairs (Figure 4A-B). In general and as
232 expected, odorant responses increased with increasing odorant concentration. All *Sfla* Or67b paralogs
233 had similar dose-response-curves when stimulated with BITC, while other ITCs elicited Or-specific
234 dose-responses (Figure 4). All three *Sfla* Or67b paralogs are sensitive to ITCs, responding to relatively
235 low odorant concentrations, but have differential ITC selectivity. Lastly, we analyzed the responses of
236 the three *Sfla* Or67b paralogs using principal component analysis (PCA). We found that most ITC
237 responses distributed separately in the odor space when OSNs were tested at 1:100 vol/vol, except for
238 BITC, 4MBITC and 3MPITC, which were separated best at 1:1,000 vol/vol (Figure supplement 4).

239 We next tested the extent to which the presence of the ITC functional group ($-N=C=S$) was
240 necessary for evoking responses from OSNs expressing *Sfla* Or67b paralogs. Therefore, we stimulated
241 OSNs with each of two linkage isomers, BITC (which bears the ITC functional group, $-N=C=S$) and
242 benzyl thiocyanate BTC (which bears the thiocyanate functional group, $-S\equiv C-N$) (Figure 3B, C).
243 Stimulation with BITC produced robust activity in OSNs expressing any of the three paralogs (one-
244 sample signed rank tests, $p<0.05$), while stimulation with BTC had no effect ($p>0.05$; Figure 3B, C).
245 This differential activation pattern is therefore likely due to the presence of different functional groups
246 (ITC vs. TC), because these compounds are not only isomers but also have similar volatilities.

247

248 ***S. flava* antennal OSNs are responsive to ITCs**

249 *Sfla* Or67b paralogs responded sensitively to diverse ITCs when expressed in the heterologous
250 empty neuron system (Figure 4). We next investigated whether ITC-sensitive Ors are indeed present in
251 the antenna of *S. flava* by recording olfactory responses of *S. flava* antennal basiconic-like (n=36 OSNs)
252 and trichoid-like sensilla (n=36 OSNs: Figure supplement 5) to stimulation with BITC 1:1,000 vol/vol.
253 We used BITC at this low, naturally-occurring concentration, because it evoked responses from all *S.*

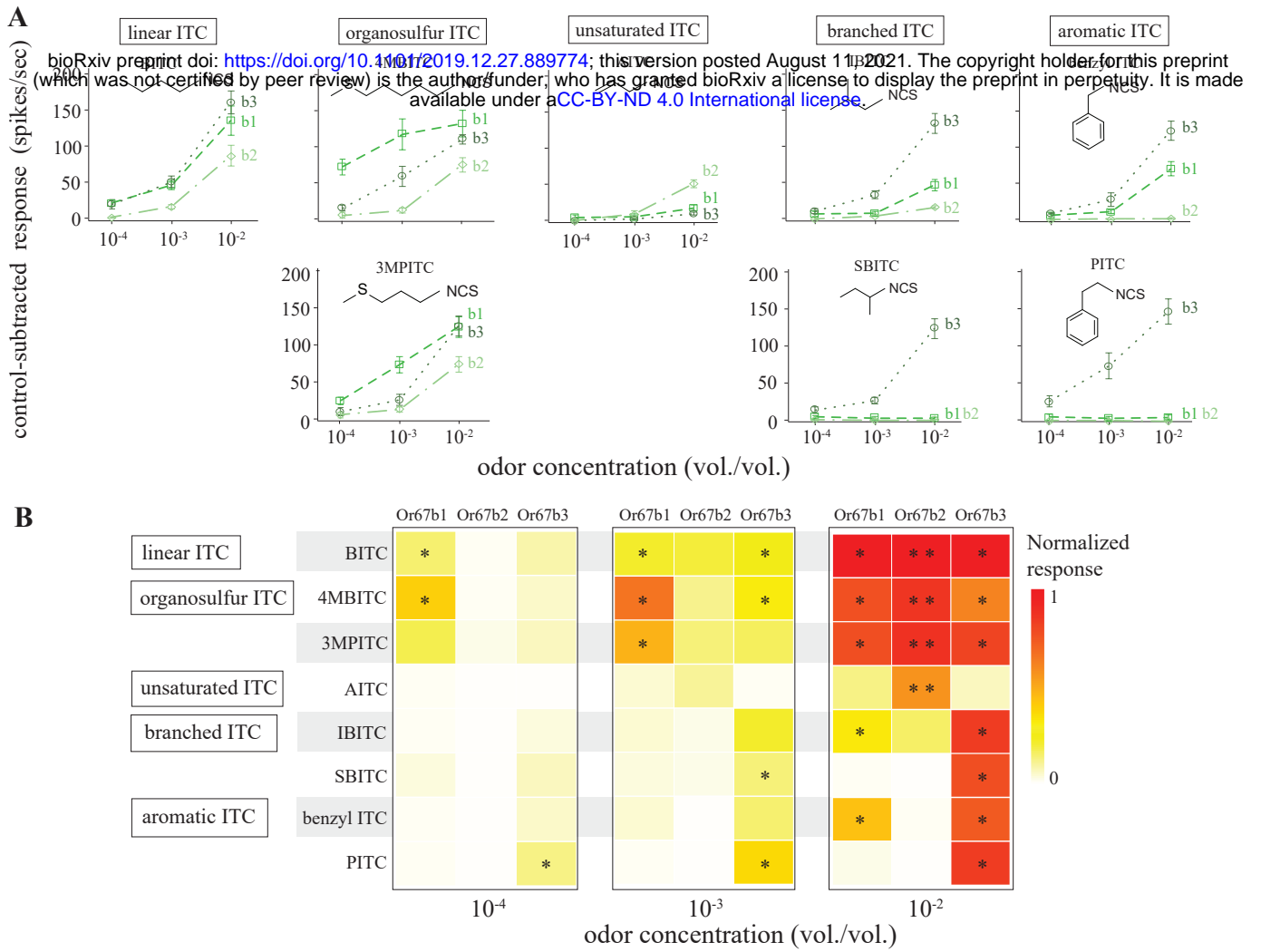


Figure 4 *Sfla* Or67b1-3 have distinct ITC selectivity.

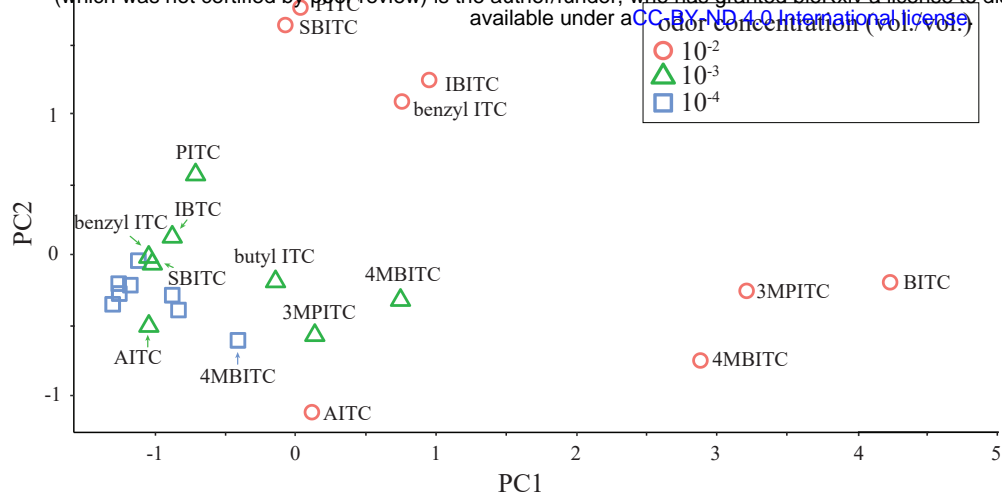


Figure supplement 4 Principal component analysis (PCA) of median responses from the three *S. flava* paralogs

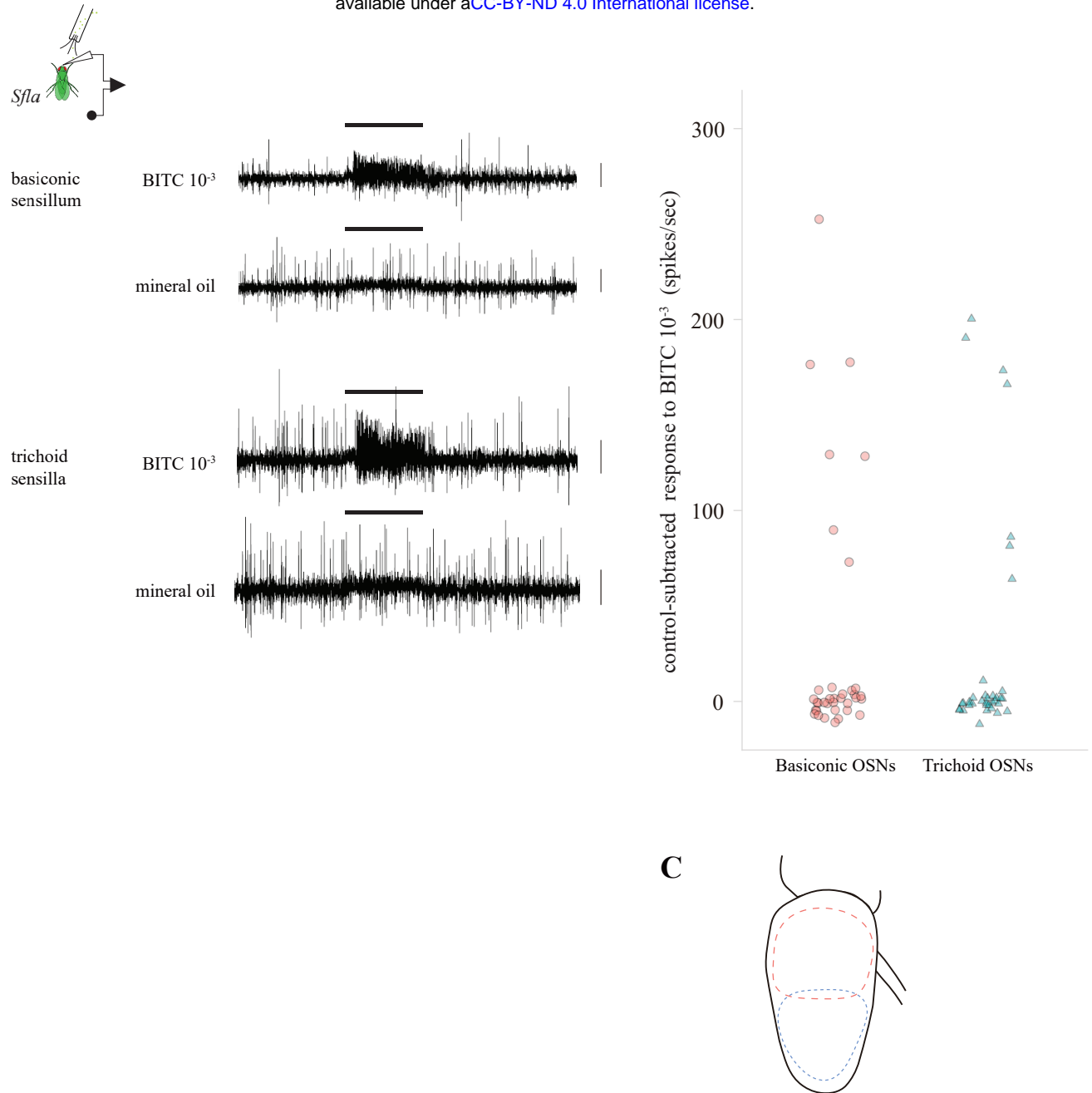


Figure supplement 5 Antennal OSNs respond to ITCs in *S. flava*.

254 *flava* paralogs (Figure 4B; middle panel). We found that 19% of recorded OSNs in basiconic-like and in
255 trichoid-like sensilla showed medium to strong responses (median: 130 and 166 net spikes/second,
256 range: 74-252 and 65-200 net spikes/second respectively in each sensilla type) to stimulation with BITC
257 (Figure supplement 5A, B). These ITC-sensitive OSNs are located proximally in basiconic-like sensilla,
258 and distally in trichoid-like sensilla (Figure supplement 5C). The fact that *S. flava* has BITC-sensitive
259 OSNs in at least two different morphological types of antennal olfactory sensilla comports with our
260 finding that *Sfla* Or67b2 is functional only when expressed in trichoid sensilla of *D. melanogaster*, while
261 *Sfla* Or67b1 and *Sfla* Or67b3 are functional in basiconic sensilla of *D. melanogaster*.

262

263 ***S. flava* is attracted to mustard plant odors and volatile ITCs**

264 Because *S. flava* is a mustard plant specialist, and because we showed that *S. flava* Or67b
265 paralogs – but not those from its generalist relatives – respond selectively to ITCs, we hypothesized that
266 *S. flava* has evolved attraction to these odorants. We addressed this using a dual-choice olfactory assay
267 (based on ref. ⁶⁴; Figure 5A; Figure supplement 6) in which flies are allowed to choose between and
268 odor-laden and an odorless arm of a “y-maze” olfactometer ³⁷.

269 We first tested the extent to which flies are differentially attracted to mustard and non-mustard
270 leaf VOCs under our experimental conditions. *S. flava* is attracted to arugula and *A. thaliana* leaf VOCs
271 (two-tailed Binomial tests, in all cases $p < 0.05$), while the closely related species *S. pallida* was not
272 ($p > 0.05$; Figure 5 and Figure supplement 7). Leaf VOCs from a non-mustard plant (e.g. tomato) did not
273 attract or repel *S. flava* ($p > 0.05$), but attracted *S. pallida* ($p < 0.01$; Figure 5), which comports with the
274 fact that *S. pallida* can be reared in medium containing decaying tomato in the laboratory. *S. flava* tested
275 with leaf VOCs from *A. thaliana* GKO and *PAD3* mutants (which differ in their ability to produce ITCs

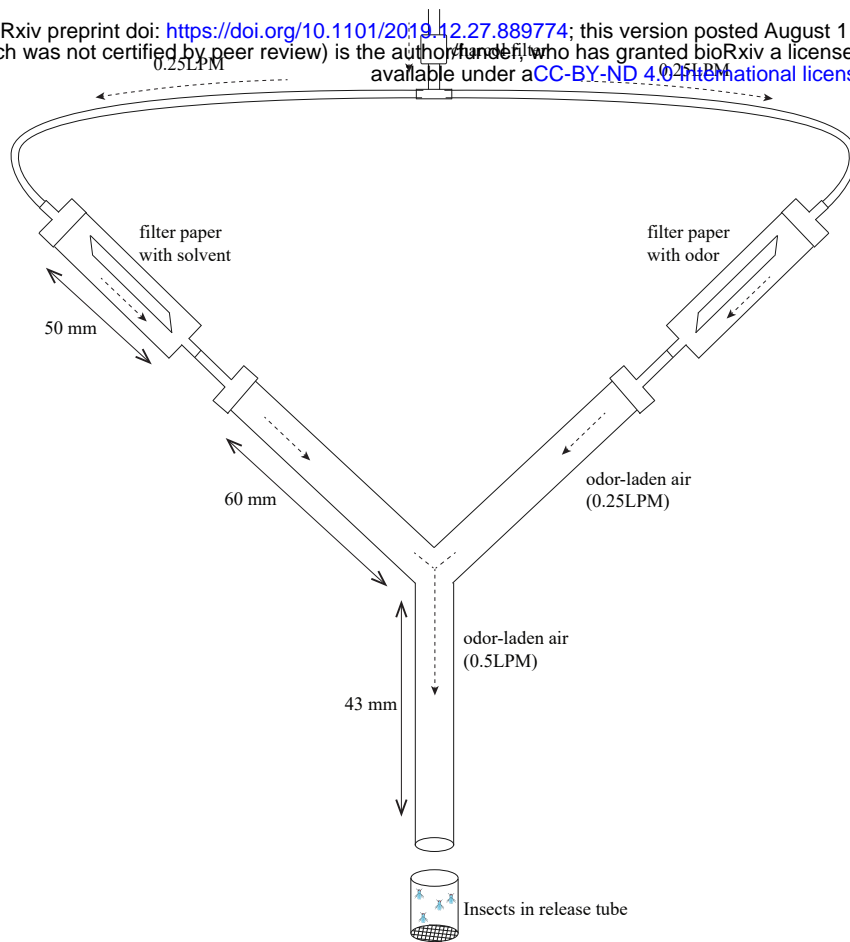


Figure supplement 6 Detailed schematic representation of the device used to test olfactory behavioral responses.

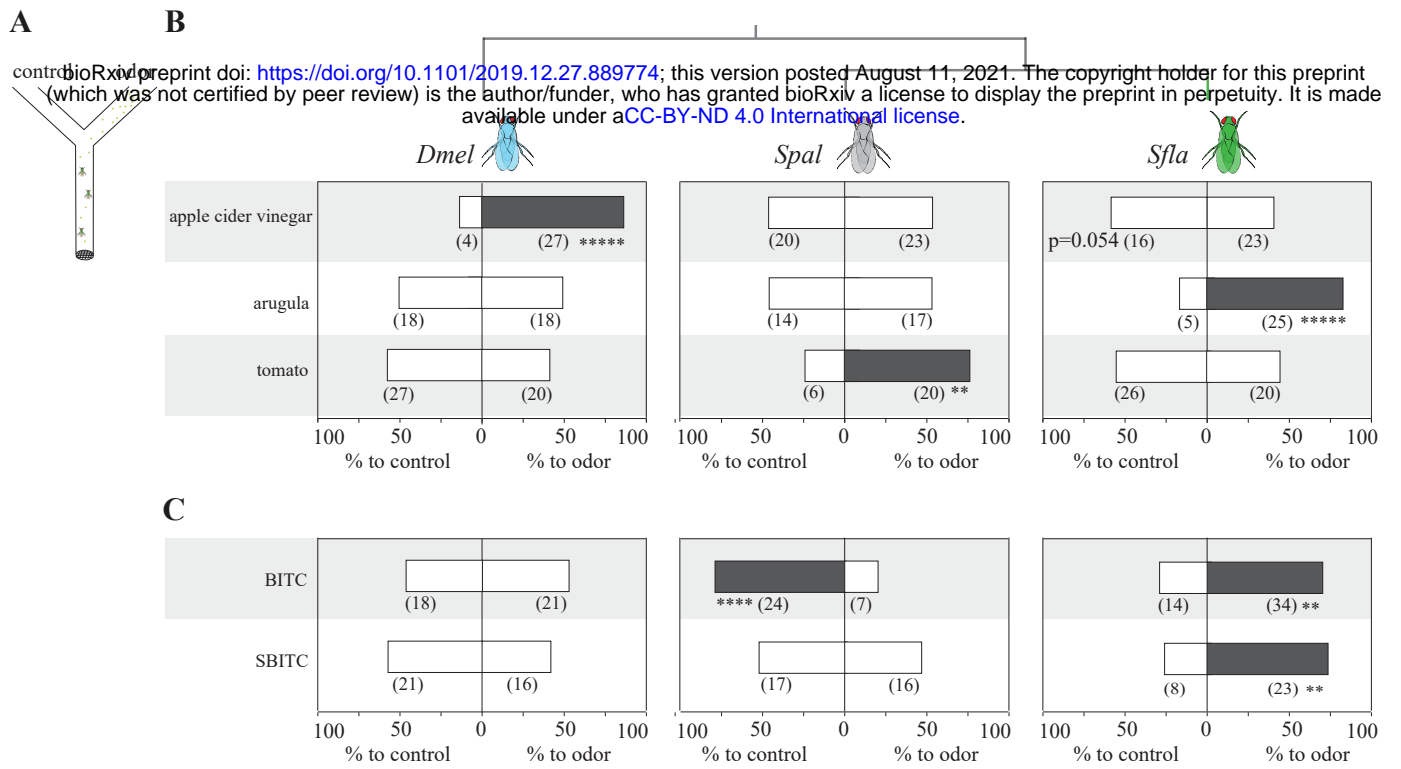


Figure 5 Olfactory behavioral responses of *S. flava* and its microbe-feeding relatives *S. pallida* and *D. melanogaster* to ecologically related odors and ITCs.

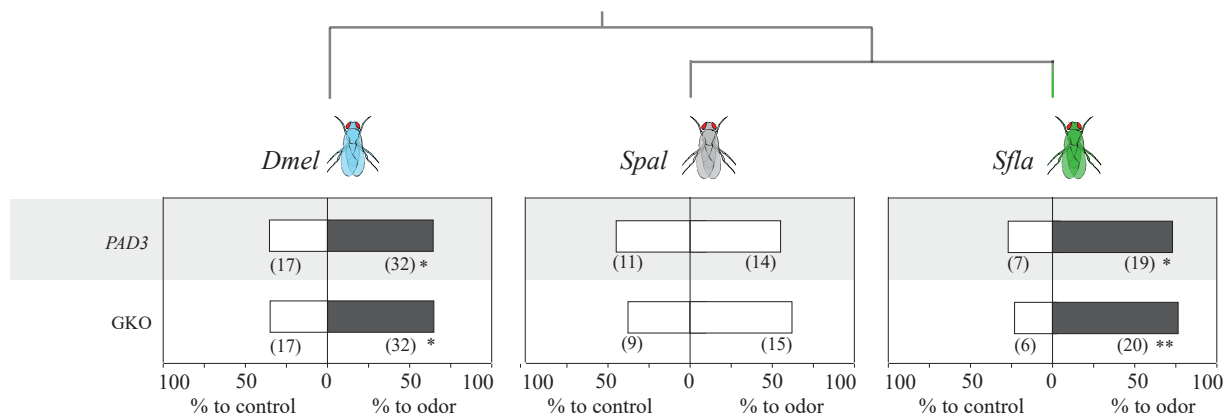


Figure supplement 7 Olfactory behavioral responses of *S. flava* and its microbe-feeding relatives *S. pallida* and *D. melanogaster* to *Arabidopsis*.

276 ^{50,52-53}) similarly preferred leaf VOCs from either of these genotypes over clean air (Figure supplement
277 7). This is not especially surprising because GKO plants still release many VOCs ⁵⁰⁻⁵³.

278 As expected, *D. melanogaster* was strongly attracted to apple cider vinegar odors ($p < 0.05$;
279 Figure 5) in agreement with previous studies ⁴⁷. Both *S. flava* and *S. pallida*, in contrast, distributed at
280 random between the apple cider vinegar odor-laden and the odorless arm of the maze (Figure 5). *S. flava*
281 is specifically attracted to mustard plant odors, but not to plant odors in general (represented by those
282 from tomato leaves), and was indifferent to odor sources that attract *D. melanogaster*, characterized by
283 acetic acid and ester, carbonyl, and hydroxyl-containing compounds ⁶⁵⁻⁶⁶.

284 We next investigated whether ITCs alone can mediate olfactory attraction in *S. flava*. We chose
285 BITC and SBITC because these compounds evoked distinct odor responses from *Sfla* Or67b paralogs
286 (Figure 4; BITC strongly activates all *S. flava* paralogs, while SBITC activates only *Sfla* Or67b3). *S.*
287 *flava* was attracted to BITC and SBITC ($p < 0.05$ in both cases; Figure 5B). Interestingly, *S.*
288 *pallida* strongly avoided BITC ($p < 0.005$; Figure 5), which must occur *via* an Or67b-independent
289 olfactory pathway because *Spal* Or67b does not respond to any of the ITCs tested, even at high
290 concentrations (Figure 3). Thus, single ITCs compounds, which evoke strong responses from *Sfla* Or67b
291 paralogs and *S. flava* antennal OSNs (Figures 3-4; Figure supplement 5), mediate olfactory orientation in
292 *S. flava* but do not attract (and can even repulse) its microbe-feeding relatives.

293

294 **Expression of *Sfla* Or67b in the homologous olfactory circuit of *D. melanogaster* confers** 295 **behavioral responses to ITCs**

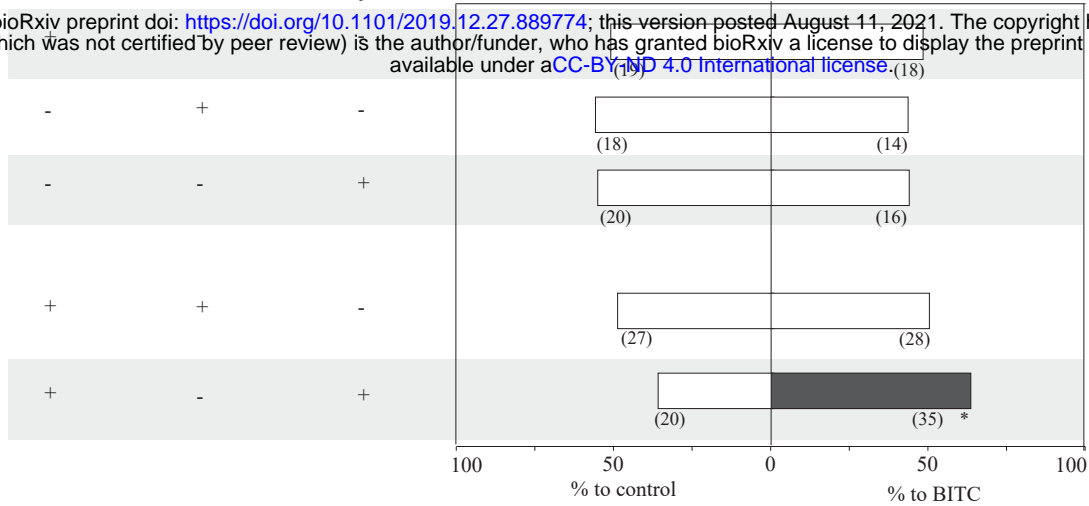
296 Because *Sfla* Or67b paralogs selectively respond to ITCs, we tested if the ectopic expression of
297 these receptors in the homologous olfactory circuit of the microbe-feeder species is sufficient to mediate
298 attraction to these compounds. We first used the Or22a olfactory circuit because it is a circuit known to

299 mediate olfactory attraction in diverse drosophilids^{32-33,67}. We focused on *Sfla* Or67b3, as this Or has a
300 broader sensitivity to ITC compounds than *Sfla* Or67b1 or *Sfla* Or67b2 (Figures 3 and 4). As before, we
301 used a dual-choice olfactometer and tested flies in which the expression of *Sfla* Or67b3 or *Dmel* Or67b
302 is under the control of GAL4 in the ab3A neuron, as well as the three parental control lines. We tested
303 flies with BITC 1:1,000 vol/vol to avoid compensatory/un-specific responses caused by the lack of
304 Or22a. *D. melanogaster* flies expressing *Sfla* Or67b3, but not *Dmel* Or67b in ab3A OSNs, preferred the
305 BITC-bearing arm of the maze ($p < 0.05$, Figure 6A). Having found that ectopic expression of an Or
306 confers behavioral responses in this set-up, we next expressed *Sfla* Or67b3 in the Or67b-expressing
307 homologous olfactory circuit of *D. melanogaster* (in this experiment flies did not lack expression of the
308 endogenous Or67b). Flies expressing this Or, but not those expressing an additional copy of *Dmel*
309 Or67b (a control), were attracted to BITC ($p < 0.05$; Figure 6B). Ectopic expression of the ITC-
310 responsive *Sfla* Or67b3 in the homologous Or67b circuit of the distantly related (*ca.* 70 million years
311 divergence time) microbe-feeding *D. melanogaster* can confer olfactory responses to ITCs.

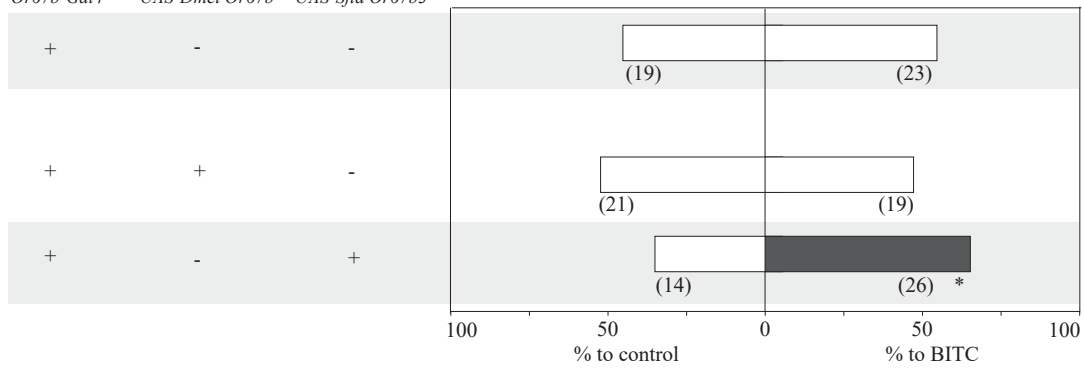
312 These results provide an experimental test of the extent to which the Or67b olfactory circuit
313 mediates olfactory attraction in *D. melanogaster*, as has been found for *D. mojavensis*⁴⁴. To address
314 this, we took advantage of the high sensitivity of *Dmel* Or67b to acetophenone (Figure 3 and ref.⁵⁵),
315 which evokes behavioral attraction at low concentrations but repellence at high concentrations⁶⁸. Our
316 experimental conditions faithfully reproduced these results: *D. melanogaster* (Canton-S) was attracted to
317 low concentrations of acetophenone and repelled by high concentrations (Figure supplement 8). Further,
318 we silenced Or67b OSNs using UAS-Kir2.1, an inwardly-rectifying potassium channel that suppresses
319 neuronal activity⁶⁹ under the control of Or67b-Gal4. Genetic controls showed a tendency for attraction
320 to low concentrations of acetophenone (63% in both cases; $p = 0.052$ and 0.077 ; Figure 6C), while flies
321 with Or67b OSNs silenced were repelled (Figure 6C; Binomial test, $p < 0.05$). The *D. melanogaster*

A *Or22a-Gal4* *UAS-Dmel Or67b* *UAS-Sfla Or67b3*

bioRxiv preprint doi: <https://doi.org/10.1101/2019.12.27.889774>; this version posted August 11, 2021. The copyright holder for this preprint (which was not certified by peer review) is the author/funder, who has granted bioRxiv a license to display the preprint in perpetuity. It is made available under aCC-BY-ND 4.0 International license.



B *Or67b-Gal4* *UAS-Dmel Or67b* *UAS-Sfla Or67b3*



C *Or67b-Gal4* *UAS-Kir2.1*

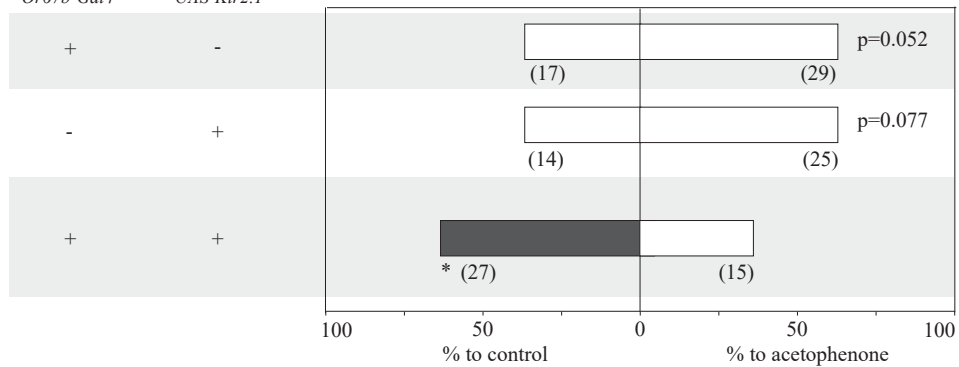


Figure 6 Ectopic expression of *Sfla Or67b3* in Or22a OSNs or Or67b OSNs conferred behavioral responses to BITC in *D. melanogaster*.

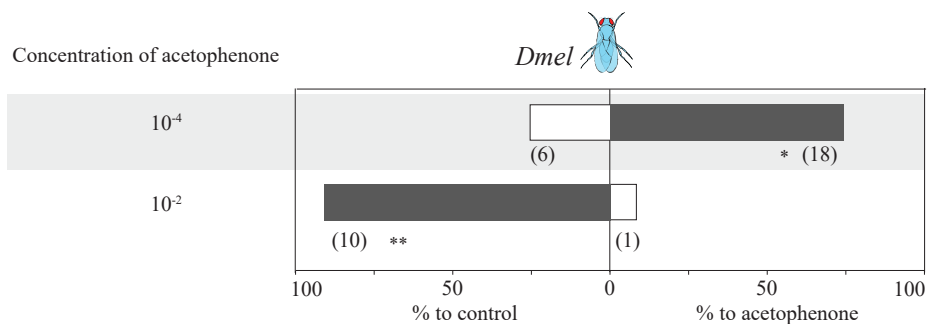


Figure supplement 8 Concentration-dependent behavioral responses of wild-type *D. melanogaster* to acetophenone

322 Or67b olfactory circuit mediates attraction towards low concentrations of a cognate ligand. Aversion to
323 low concentrations of acetophenone in flies with Or67b OSNs inactivated is likely due to activation of
324 other Ors sensitive to this odorant (e.g. Or10a⁵⁵) which mediate odorant repulsion. Activation of OSNs
325 in the *D. melanogaster* Or67b olfactory circuit is necessary for behavioral orientation towards Or67b
326 cognate ligands (i.e. acetophenone), whereas this activation is sufficient to confer orientation towards
327 ligands of ectopically expressed Ors (e.g. ITCs). Simple evolutionary changes in the odorant tuning of
328 an Or (from acetophenone to ITCs) can change the identity of the odorants (in this case ITCs) that evoke
329 behavioral responses³⁷⁻³⁸. It remains to be investigated whether putative downstream changes in Or67b
330 circuitry³⁸ occurred in *S. flava*.

331

332 **DISCUSSION**

333 Most herbivorous insect species specialize on a narrow range of host plant species⁷⁰ that
334 synthesize similar secondary compounds. While these toxins serve to defend against herbivory,
335 ancestrally aversive molecules can become co-opted as attractants to those herbivores that specialize on
336 a particular toxic host plant lineage. We investigated the genetic and functional mechanisms underlying
337 the evolution of attraction to toxic host-plants using *S. flava* as a model. A candidate Or lineage (*Or67b*)
338 was triplicated in a recent ancestor of *S. flava* and experienced rapid protein evolution, resulting in three
339 divergent paralogs (*Sfla Or67b1-b3*; Figure 1). Each *Sfla Or67b* paralogs specifically responded to
340 stimulation with mustard-plant odors and volatile ITCs in heterologous expression systems (Figures 2
341 and 3) and to a specific subset of ITCs (Figure 4). In contrast, *S. pallida* and *D. melanogaster Or67b*
342 orthologs did not respond to ITCs but showed strong responses to stimulation with apple cider vinegar
343 and a broad range of aldehydes, alcohols and ketones (Figures 2 and 3), consistent with their microbe-
344 feeding niche⁷¹. In agreement with these results, recordings from *S. flava* antennal sensilla revealed

345 OSNs sensitive to ITCs (Figure supplement 4). *S. flava*, but not *S. pallida* or *D. melanogaster*, is
346 attracted to volatile ITC compounds (Figure 5). Ectopic expression of *S. flava* Or67b3 in the *D.*
347 *melanogaster* homologous olfactory circuit conferred odor-oriented behavioral responses to ITCs
348 (Figure 6). Finally, suppression of activity in Or67b positive OSNs in *D. melanogaster* decreased
349 preference to a *Dmel* Or67b cognate ligand, acetophenone (Figure 6). The ancestral Or67b olfactory
350 circuit therefore likely mediates olfactory attraction. Altogether, these results suggest that gene
351 duplication followed by specialization is a mechanism by which specialist herbivores evolve Ors that
352 may mediate olfactory attraction towards ancestrally aversive chemical compounds.

353

354 **Evolutionary path of olfactory receptor specialization**

355 Or67b triplication in *S. flava* raises several molecular evolutionary questions, including how this
356 duplication contributed to the generation of novel gene functions. In this regard, several scenarios have
357 been proposed^{22,72}: (A) neofunctionalization, when one of the duplicated genes (paralogs) acquires a
358 new function after accumulating *de novo* mutations, while the other copy retains ancestral function; (B)
359 subfunctionalization *sensu stricto*, where mutations accumulate in both copies leading to partitioning of
360 ancestral function; and (C) specialization, when subfunctionalization and neofunctionalization evolve
361 simultaneously, yielding gene copies that are functionally different from one another and the ancestral
362 copy⁷³⁻⁷⁴. Each *Sfla* Or67b paralog selectively responds to different subsets of ITCs across a range of
363 odorant concentrations, while the proteins from its close relatives did not respond to ITCs (Figures 3 and
364 4). Or67b evolved new ligand-binding affinities in *S. flava*, indicating a neofunctionalization event.
365 Because each paralog responds to different subsets of ITCs, this shift likely evolved before the
366 duplications of Or67b (Figure 7).

367

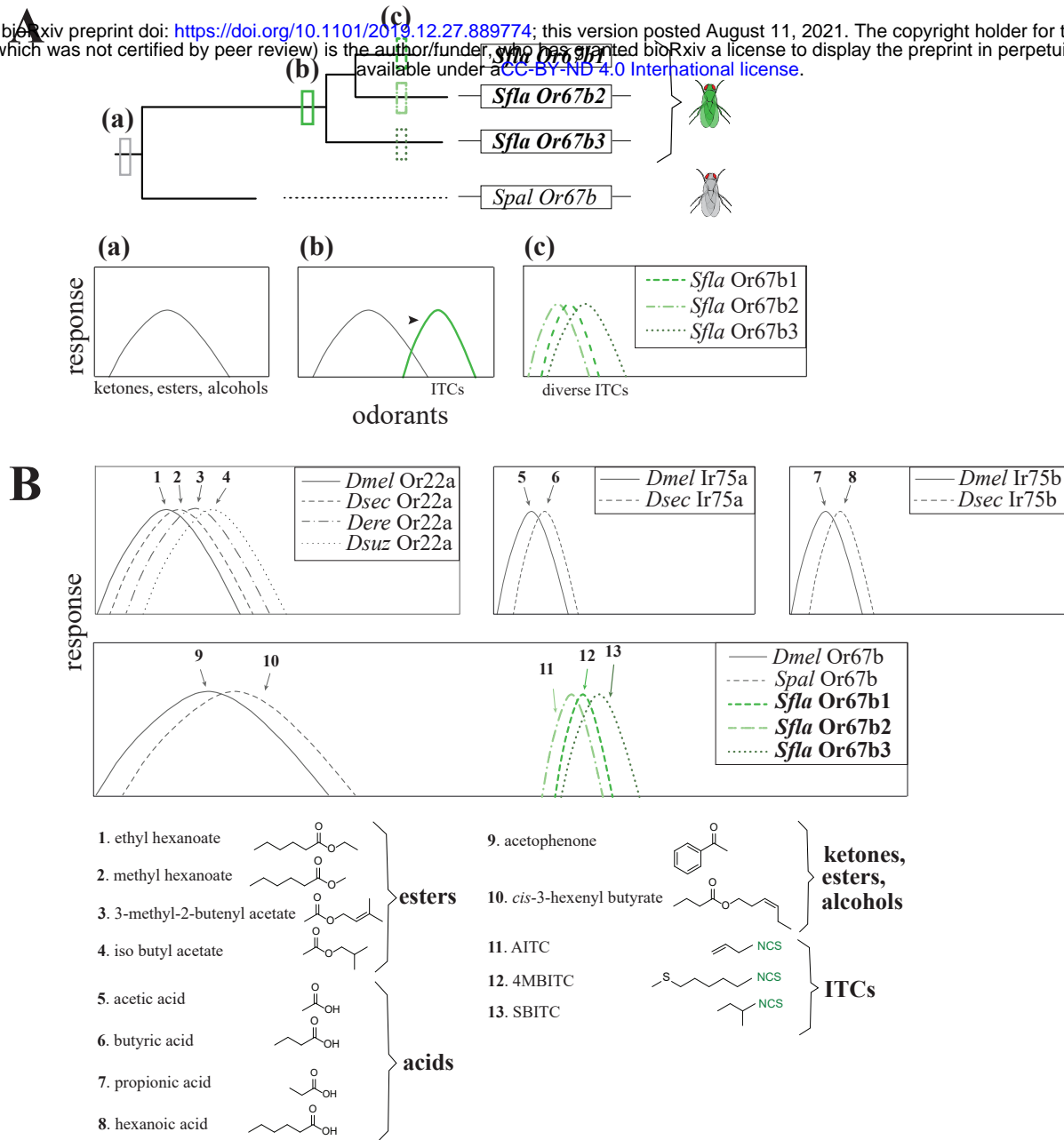


Figure 7 A model for the evolution of *Or67b* and comparison with the known evolution of other *Or* orthologs in drosophilid flies.

368 **An olfactory receptor sensitive to a new niche-specific chemical class of odorant compounds**

369 Across Drosophilidae, orthologous chemoreceptors respond in a species-specific manner to
370 ecologically relevant ligands. Or22a is a good example of a hot-spot for sensory evolution in *Drosophila*
371 because shifts in ligand binding sensitivity led to different odor-preference behaviors^{37,67}. Or22a and
372 other highly variable receptors such as Ir75a/b, typically evolve new specificities towards different
373 odorants within one chemical class⁷⁵ (Figure 7). However, this is not the case for Or67b, which
374 responds to alcohols, aldehydes and ketones in non-herbivorous *D. melanogaster* and *S. pallida*, but in
375 *S. flava*, each paralog is highly sensitive to volatile ITCs, an entirely different chemical class (Figures 3
376 and 4). The presence of the ITC functional group ($-N=C=S$) is key to activating these olfactory
377 receptors, highlighting a functional shift in ligand binding specificity (Figure 3B, C). The striking
378 difference in odor selectivity among Or67b orthologs may result from the evolution of herbivory in
379 *Scaptomyza*.

380

381 **An olfactory receptor likely mediating attraction to mustard host plants**

382 Through our use of odors produced by crushed leaves of mutant *A. thaliana*, we found that *S.*
383 *flava* has at least two different olfactory pathways for mustard-plant host attraction: ITC-dependent and
384 ITC-independent (Figure 5 and Figure supplement 7). This is consistent with the fact that plant VOCs
385 are complex bouquets of diverse, lineage-specific molecules that are variably capable of releasing
386 attraction behaviors in specialist herbivores⁷⁶. Our results do not preclude that other chemoreceptors
387 and OSNs also contribute to mediate olfactory attraction to mustard plant volatiles and ITC compounds
388 in *S. flava*. The necessity of Or67bs for orientation towards ITCs could be probed by generating *S. flava*
389 Or67b loss of function mutants and testing whether flies can still orient towards these odorants. Because
390 *S. flava* females lay eggs in the leaf mesophyll, generation of *Or67b* mutants using CRISPR-Cas9 was

391 not feasible. New technologies such as ReMOT Control⁷⁷ should enable such experiments in the future.
392 It also remains to be explored if evolution sculpted neural wiring³⁷⁻³⁸ to modulate responses to ITC
393 compounds.

394 ITC taste detection in vertebrates and insects leads to aversive behaviors mediated by the contact
395 chemoreceptor TrpA1^{2,78-79}. However, volatile ITCs are widely used to trap pests of Brassicaceae⁹. In
396 agreement with this, the antennae of some of these insects, including *S. flava*²¹ (Figure supplement 4),
397 respond to volatile ITCs^{10,80-81}. Similarly, the mustard specialist Diamondback moth *P. xylostella* uses
398 two endogenous Ors selective to ITCs¹⁰. These Ors are selective to three ITC compounds, including two
399 (3MPITC and PITC), which strongly activate *S. flava* Or67b paralogs, suggesting that these ITC
400 compounds¹⁰ are important for host-orientation in mustard specialists. Importantly, our study further
401 advanced our understanding about the mechanisms underlying evolution of ITC-detecting Ors by
402 comparing Or evolution, function and behavior in herbivorous and non-herbivorous *Scaptomyza* species.
403 The relevance of these gene duplication events is also consistent with the finding that *Or67b* is
404 duplicated only in Brassicaceae-specialist *Scaptomyza* spp.⁸² and not in other herbivorous *Scaptomyza*
405 species specialized on non-Brassicaceae hosts (*i.e.* *S. graminum*; Figure 1C). Thus, gene duplication and
406 subsequent sequence evolution has played an important role in co-evolution (*sensu lato*) between
407 Brassicaceae plants and diverse herbivorous insects that use them as hosts. More generally,
408 chemosensory specialization in herbivorous insects can result from relatively simple genetic
409 modifications in the peripheral nervous system that change olfactory receptor tuning, contributing to
410 major niche shifts.

411

412

413

414 MATERIALS AND METHODS

415 Molecular phylogeny of drosophilid olfactory Olfactory Receptors (Or)

416 Translations of *Ors* from *D. grimshawi*, *D. mojavensis*, *D. virilis* and *D. melanogaster* (builds
417 dgri r1.3, dmoj r1.3, dvir r1.07 and dmel r6.28, respectively) were downloaded from Flybase
418 (www.flybase.org; ⁸³). *S. flava* *Or* sequences were previously published ²¹. A total of 309 sequences
419 were aligned in MAFFT v7.017 with the E-INS-I algorithm and then manually adjusted ⁸⁴. Models were
420 fitted to the alignment using IQ-Tree and tested using the cAIC criterion ⁸⁵. A maximum likelihood
421 (ML) phylogeny was generated using the Or protein alignment (in RAxML v8.2.10) with the CAT
422 model of rate heterogeneity with seven distinct categories, the JTT substitution matrix, empirical amino
423 acid frequencies, and 1,000 rapid bootstraps ⁸⁶. Orco sequences were designated as the outgroup as is
424 standard practice in evolutionary analyses of arthropod Ors.

425

426 Time calibrated molecular phylogeny of *Scaptomyza* and *Drosophila* spp.

427 A time-calibrated species tree was inferred using the loci: *16S*, *COI*, *COII*, *ND2*, *28S*, *Cad-r*,
428 *Gpdh1*, *Gstd1*, *Marf*, *l(2)tid* (also known as *Alg3* or *Nltidi*) and *AdhR* from 13 spp of *Drosophila* and four
429 *Scaptomyza* spp. *Scaptomyza* sequences were accessed from the genomes in refs. ^{13,87} using tblastn
430 searches for protein coding genes and blastn searches for the ribosomal RNA genes. The *Adh Related*
431 gene appears to be deleted in *S. flava* and was coded as missing data. Two uniform priors on the age of
432 *Scaptomyza* and the age of the combined virilis-repleta radiation, Hawaiian *Drosophila* and *Scaptomyza*
433 clade were set as in ref. ⁸⁸. Protein coding genes were partitioned into first and second combined and third
434 position partitions, except *COI* and *Gpdh1*, which were divided into first, second and third partitions.
435 The partitioning scheme was chosen based on Partition Finder 2.1.1 ⁸⁹ and nucleotide substitution
436 models chosen with IQ-Tree ⁸⁵. Model parameters, posterior probabilities, accession numbers and

437 genome coordinates can be found in table 1. Five independent runs of BEAST v2.6.2⁹⁰ each with 25
438 million generations were run logging after every 2500th generation to infer the chronogram with 10%
439 burn-in. Phylogenies were also inferred in RAxML v8.2.12⁸⁶ with the GTR+GAMMA+I model and
440 1000 rapid bootstraps and with parsimony in PAUP* 4.0a⁹¹ with TBR branch swapping and 1000
441 bootstraps. Phylogeny parameters, sequence accession numbers and likelihood scores available in
442 supplementary dataset 1.

443

444 **Molecular phylogeny of drosophilid *Or67b* genes**

445 *Or67b* coding sequences (CDS) from *D. grimshawi*, *D. mojavensis*, *D. virilis*, *D. sechellia*, *D.*
446 *simulans*, *D. erecta*, *D. yakuba*, *D. pseudoobscura*, *D. persimilis*, *D. ananassae* and *D. melanogaster*
447 (builds dgri r1.3, dmoj r1.3, dvir r1.07, dsec r1.3, dsim r1.4, dere r1.3, dyak r1.3, dpse r3.2, dper r1.3,
448 dana r1.3 and dmel r6.28, respectively) were downloaded from Flybase (www.flybase.org; ⁸³) and *D.*
449 *hydei* from Genbank (accession number XM_023314350.2). The *S. pallida* DNA sequence was obtained
450 through PCR and Sanger sequencing as described below. *S. flava* DNA sequences were previously
451 published²¹. Two more *Scaptomyza* sequences were obtained from refs. ^{13,87} including the non-leaf-
452 mining species *S. hsui* (subgenus Hemiscaptomyza and a microbe-feeder) and *S. graminum* (subgenus
453 *Scaptomyza* and a leaf-miner on Caryophyllaceae). DNA sequences were aligned, partitioned by codon
454 position, models fitted to all three partitions and chosen according to AICc (GTR+I+G) in IQ-Tree⁸⁵.
455 Trees were inferred using RAxML (v8.2.10) with the GTRGAMMA+I model and 1000 rapid
456 bootstraps, and MrBayes (v3.2.6) setting Nst to 6, nucmodel to 4by4, rates to Invgamma, number of
457 generations to 125,000, burnin equal to 20% of generations, heating to 0.2, number of chains to 4, runs
458 to 2 and priors set to default setting⁹². An additional parsimony analysis was performed in Paup 4.0⁹¹

459 with TBR branchswapping and 1000 bootstraps. Model parameters, accession numbers and likelihood
460 scores available in Supplementary file 1.

461

462 **Analysis of molecular evolutionary rates**

463 CDS of homologs of every *Or* gene in *S. flava* found in the twelve *Drosophila* genome builds
464 were aligned to *S. flava Or* CDS. Homology was assessed according to inclusion in well-supported
465 clades in the *Or* translation phylogeny from the twelve species; *S. flava* sequences were previously
466 published²¹. Sequences were aligned in MAFFT (v7.017)⁸⁴ and adjusted manually to preserve codon
467 alignments. *Or98a*-like genes found in subgenus *Drosophila* species were split into three separate
468 clades, as were a group of *Or83c* paralogs not found in *D. melanogaster*, and a group of *Or85a*-like
469 genes. All examined sequences of *Or46a* contain two alternatively spliced exons, so this gene was
470 analyzed with all gene exon sequences in a single alignment. *Or69a*, however, contains alternatively
471 spliced exons only in species within the subgenus *Sophophora*, and therefore these alternative splice
472 forms were analyzed as separate taxa. Phylogenies were generated for every alignment using PhyML⁹³
473 with the GTR+G substitution models. If >70% bootstrap support was found for a topology contrary to
474 the known species topology, or if the *Or* homology group contained duplicates, these trees were used in
475 PAML analyses instead of the species tree.

476 Our next goal was to identify *Or* genes experiencing rapid rates of protein evolution. Branch
477 models of sequence evolution were fit using PAML 4.9h⁴¹. A foreground/background branch model
478 was fit for every *S. flava* tip branch and every ancestral branch in a *Scaptomyza*-specific *Or* gene
479 duplication clade, and compared in a likelihood ratio test to a null model with one d_N/d_S rate (ratio of
480 non-synonymous to synonymous substitution rate) for every unique phylogeny (75 tests in total). After
481 focusing on *Or67b*, patterns of molecular evolution among the drosophilid *Or67b* homologs were

482 explored using the expanded *Or67b* CDS phylogeny above. Foreground/background branch models
483 were fit for every branch in the *Or67b* phylogeny and the *S. flava* *Or67b* paralogs clade with likely ratio
484 tests performed as above (34 tests total, table 2). P-values were adjusted for multiple comparisons using
485 the false-discovery rate (FDR) method⁹⁴. Branch test results and model parameters in Supplementary
486 file 2.

487

488 **Synteny analysis between *S. flava*, *S. pallida* and *D. melanogaster Or67b* scaffolds**

489 Five genes up and downstream of each *Or67b* ortholog in *S. flava* were extracted using
490 annotations from a current GenBank assembly (GenBank Assembly ID GCA_003952975.1), shown in
491 Supplementary file 2. These genes are respectively known as pGOIs (genes proximal to the gene of
492 interest, or GOI). To identify pGOIs, we used tBLAST to the *D. grimshawi* genome, the species closest
493 to *S. flava* with a published annotated genome (GenBank Assembly ID GCA_000005155.1). By
494 identifying the pGOI scaffolds, we determined that there was only one copy of *Or67b* in *D. grimshawi*,
495 which is syntenic with the *S. flava Or67b2* ortholog. We determined that this copy is also syntenic with
496 the single *Or67b* copy of *S. pallida* (Figure supplement 2) and *D. melanogaster*.

497

498 **Fly husbandry and lines**

499 *D. melanogaster* (wild-type Canton-S and transgenic lines) were reared using standard cornmeal
500 media, yeast, and agar medium prepared by UC-Berkeley core facilities. Isfemale lines of *S. pallida*
501 (collected in Berkeley, California, US) were maintained on Nutri-Fly medium (Genesee Scientific). *S.*
502 *flava* (collected in New Hampshire, US) were maintained on fresh *A. thaliana* plants and 10% honey
503 water solution. All flies were cultured at 23°C and 60% relative humidity under a 12-h light/12-h dark

504 cycle. *S. flava* and *S. pallida* were ca. 7-10 days old at the time of experiments; *D. melanogaster* (wild-
505 type or transgenic) were ca. 3-10 days old at the time of the experiments.

506 Flies used for heterologous expression of Ors were of the following genotypes: for flies with
507 ab3a “empty neuron” system, *Or22ab^{Gal4::3xP3-DsRed}* was used. This “M2-MD” line was generated by a
508 CRISPR-Cas9 mediated deletion of *Or22a/b* and a knock-in of *Gal4* and *DsRed*⁹⁵ by homology directed
509 repair (HDR); in these flies *Gal4* is not functional. Therefore, we used *Or22ab^{Gal4::3xP3-DsRed}*; *Or22a-*
510 *Gal4/UAS-Or67b* flies were used for experiments. For flies with the at1 “empty neuron” system,
511 *Or67d^{Gal4}* line²⁸ was used. The functional absence of *Or22a* and *Or22b* genes in M2-MD flies, or
512 functional absence of *Or67d* in the *Or67d^{GAL4}* line, were respectively confirmed by electrophysiological
513 analysis on ab3A neurons or at1 neurons (Figure supplement 3). The M2-MD line was used to generate
514 flies expressing *Dmel Or67b*, *Spal Or67b*, *Sfla Or67b1* and *Sfla Or67b3* under the control of *Gal4* in the
515 ab3A “empty neuron”⁴⁶. Similarly, the *Or67d^{GAL4}* line was used to generate flies expressing *Sfla*
516 *Or67b2* under the control of *Gal4* in the at1 “empty neuron”²⁸. The progeny of those crosses was then
517 used for single sensillum recordings and in some cases for behavioral assays. The *UAS-SflaOr67b1*,
518 *UAS-Sfla Or67b2*, *UAS-Sfla Or67b3*, and *UAS-Spal Or67b* strains were generated during this study. The
519 *Or67b-Gal4* fly line (BDSC# 9996) was crossed with *UAS-Or67b* lines or *UAS-Kir2.1*⁶⁹ for behavioral
520 assays.

521

522 ***Scaptomyza Or67b* gene cloning, UAS line generation, and verification of *S. flava Or67b***

523 **transcription**

524 The *UAS-Or67b* transgene lines were constructed as follows: RNA was extracted from 20–25
525 days post-emergence adults of both sexes from laboratory-reared *S. pallida* (collected from the White
526 Mountains, New Mexico, USA) and *S. flava* (collected from near Portsmouth, New Hampshire, USA).

527 RNA was extracted using Trizol (Thermo-Fisher, Waltham, MA, USA) and precipitated with
528 isopropanol. Extracted RNA was treated with DNaseI, cDNA was generated using qScript cDNA
529 Supermix (Quantabio, Beverly, MA, USA). Absence of genomic DNA in cDNA preparations was
530 verified by attempting to PCR-amplify fragments of the *Marf* gene from reactions lacking reverse
531 transcriptase (Source data). PCR conditions and primers are detailed in ¹². CDS plus 7–9 bp of
532 untranslated sequence were amplified using High Fidelity Phusion Taq (New England BioLabs, NEB,
533 USA), 3% DMSO vol/vol, and the PCR primers (Supplementary file 4) with the following program:
534 initial denaturing at 98°C during 30 sec; 35 cycles at 98°C during 10 sec, 58°C during 30 sec, 72°C
535 during 45 sec, and extension at 72°C during 7 min. PCR fragments of the expected size were purified
536 using the Qiaquick Gel purification kit protocol (Qiagen). An overhang was added to purified *Or67b*
537 amplicons with Taq polymerase (Fermentas) and cloned using the pGEM-T Easy cloning kit protocol
538 (Promega). Plasmids were extracted and purified using the GenElute plasmid miniprep kit (Sigma-
539 Aldrich, St. Louis, MO, USA). EcoRI and KpnI cut sites were introduced using restriction enzyme cut-
540 site primers (Supplementary file 3) with 10 ng/μL diluted plasmids (as template) with 3% DMSO
541 vol/vol and the following program: initial denaturing at 98°C during 30 sec; 35 repetitions of 98°C
542 during 10 sec, 55°C during 50 sec; 72°C during 45 sec; and final extension at 72°C during 7 min. The
543 pUAST attB plasmid ⁹⁶ and the four *S. pallida* and *S. flava Or67b* PCR amplicons with RE flanking sites
544 were individually double-digested with KpnI and EcoRI high-fidelity enzyme in cut smart buffer for 3
545 hours, according to the manufacturer's protocol (NEB). Cut fragments were gel-purified using the
546 Qiaquick Gel Cleanup Kit (Qiagen) and ligated in a 1:3 vector:insert molar ratio using T4 ligase
547 (Promega). Ligations were transformed into JM109 cells. Some cells were preserved as glycerol stocks
548 and a portion were used for injection into the $y^1 w^{67c23}$; P{CaryP}attP2 *D. melanogaster* line for
549 generating *Sfla Or67b1*, *Sfla Or67b2*, *Sfla Or67b3*, *Spal Or67b* or into the $y^1 w^{67c23}$; P{CaryP}attP40 for

550 *Sfla Or67b2* (BestGene Inc., Houston, Texas, USA). Transformants were selected from individually
551 injected flies with compound eye color rescue phenotypes.

552

553 **Single sensillum recordings (SSR)**

554 All *Or67b* constructs were expressed in the ab3A empty neuron system, except *Sfla Or67b2*,
555 which was expressed in at1 empty neuron system because this Or exhibited spontaneous activity only in
556 at1 trichoid OSNs in transgenic *D. melanogaster* flies (Figure supplement 3).

557 Fed, adult female flies were prepared for SSR as previously described⁴⁵. We identified the
558 antennal sensilla housing the OSN(s) of interest using an Olympus BX51 WI upright microscope with
559 10x and 50x objectives (Olympus, UPlanFL N 10x, UplanFL N 50x). We recorded the responses of 6-10
560 sensilla obtained from 2-4 individuals for each experiment/odorant, the standard in this type of
561 experiment (e.g. ref.⁹⁷). Extracellular activity was recorded by inserting a tungsten electrode into the
562 base of either ab3 or at1 sensilla. Signals were amplified 100x (A-M systems, Differential AC Amplifier
563 model 1700), digitized using a 16-bit analog-digital converter, filtered (low cut-off: 300 Hz, high cut off:
564 500 Hz), and analyzed off-line using WinEDR (v3.9.1; University of Strathclyde, Glasgow). A tube
565 delivering a constant flow of charcoal-filtered air (16 ml/min, using a flowmeter; Gilmont instruments,
566 USA) was placed near the fly's head, and the tip of the stimulation pipette (50 ml) was inserted into the
567 constant air stream. The stimulation pipette contained a piece of filter paper loaded with 20 µl of odorant
568 solution or the solvent control. One second pulse of clean air was delivered to the stimulus pipette using
569 a membrane pump operated by a Stimulus Controller CS 55 (Syntech, Germany). Ab3 sensilla were
570 identified by using three standard diagnostic odorants⁹⁸ (all odorants were obtained from Sigma-
571 Aldrich, US, purity > 95%): ethyl hexanoate (CAS # 123-66-0), ethyl acetate (CAS # 141-78-6) and 2-
572 heptanone (CAS # 110-43-0) (Figure supplement 3). We were able to distinguish at1 sensilla from at2

573 and at3 because the former houses a OSN, whereas at2, at4 and at3 respectively house two, three and
574 three OSNs ⁹⁸.

575 The following odor sources (purchased from Berkeley Bowl in Berkeley, California, USA,
576 unless otherwise mentioned; 20 µl of material were loaded on filter paper unless noted) were used: apple
577 cider vinegar (40 µl, O Organics, USA), grated roots of the four Brassicaceae species; *W. japonica*
578 (wasabi), *A. rusticana* (horseradish), *B. rapa* (turnip), *R. sativus* (daikon), and the Amaranthaceae
579 species *B. vulgaris* (beet). Approximately 10 g of roots were grated immediately before experiments and
580 used right away to prevent compound degradation. Brassicaceae species *E. vesicaria* (arugula), *A.*
581 *thaliana*, and a Solanaceae species, *S. lycopersicum* (tomato), were grown from seeds at 23°C and 60%
582 relative humidity under a 12-hour light: 12-hour dark cycle, and leaves from 3-8 weeks old plants were
583 used for odor stimulation. The following *A. thaliana* genotypes were used: wild-type (Col-0),
584 glucosinolate knockout (GKO) mutant in *myb28 myb29 cyp79b2 cyp79b3*, which has no detectable
585 aliphatic and indolic glucosinolates nor camalexin ^{50,52-53}, and camalexin-deficient *phytoalexin deficient*
586 *3 (PAD3)* mutants that have wild-type levels of aliphatic and indolic glucosinolates (but no camalexin).
587 Therefore, *PAD3* plants are more appropriate controls for comparisons with GKO plants than Col-0
588 plants ⁵⁴. Three-four leaves were excised from plants and homogenized with a grater immediately before
589 tests; the homogenate was replaced every 30 min since OSN odor responses were stable at least during
590 this time window. All synthetic odorants were diluted in mineral oil (1:100 vol/vol) unless otherwise
591 noted. The following odorants (all from Sigma-Aldrich, US, purity >95%) were diluted in dimethyl
592 sulfoxide (DMSO): mandelonitrile (CAS # 532-28-5), iodoacetamide (CAS # 144-48-9), N-
593 methylmaleimide (CAS # 930-88-1), N-hydroxysuccinimide (CAS # 6066-82-6), and benzyl thiocyanate
594 (CAS # 3012-37-1). 11-*cis* vaccenyl acetate (CAS # 6186-98-7) and 4MBITC (CAS # 4430-36-8) were
595 diluted in ethanol. All chemicals used in this study are listed in supplementary file 6.

596 The “net number of spikes” was obtained by counting the number of spikes originating from the
597 OSN of interest during a 1-second window which started 0.2 seconds after the onset of stimulation, and
598 subtracting from this number the background spiking activity (obtained by counting the number of
599 spikes in a 1-second window prior to the onset of the odor stimulation). In all figures (unless otherwise
600 noted) the net response to each odor or odorant stimulation was subtracted from the median net response
601 to the solvent control used (some odorants were dissolved in solvents other than mineral oil, see
602 preceding paragraph).

603 In SSR experiments it is common to observe unspecific, slight increases/decreases in spiking
604 activity which are not considered biologically meaningful, including small responses to solvent controls.
605 Accordingly, it is not uncommon to find reports, including investigations using the empty neuron system
606 of *D. melanogaster*⁹⁷, in which net spiking responses smaller than 10-25 spikes/second are not
607 considered true odor-evoked responses (*e.g.*⁹⁹⁻¹⁰⁰). Therefore, we asked if the net responses to a given
608 combination of Or and odorant compound are statistically significant ($p < 0.05$) using one-sample signed
609 rank tests under the following null and alternative hypotheses:

610 *H₀*: net number of spikes > -10 and < 10

611 *H_a*: net number of spikes < -10 or > 10

612 Data were also analyzed using Mann-Whitney U tests for comparing two independent groups,
613 Kruskal-Wallis ANOVAs for comparing more than two independent groups (followed by post-hoc tests
614 if significant), and Wilcoxon-matched pairs tests for comparing two paired groups. Although results
615 were considered significant only if $p < 0.05$, we indicated cases in which p-values were slightly larger
616 ($0.05 < p < 0.08$). We informed these values because “a result that does not meet the $p < 0.05$ threshold
617 should not be considered meaningless”¹⁰¹ (specially with low sample sizes due to the nature of the

618 experiment, as in this report) “when in fact provides...at least preliminary evidence that requires further
619 attention”¹⁰¹.

620 Tuning curves and kurtosis values were generated and calculated in Microsoft Excel (2016).
621 Similarly, a matrix of median responses (control-subtracted) was produced and used for PCA in R
622 statistical software. For generation of the heatmap in R (Figure 4B), the median responses of OR-
623 odorant pairs were normalized to the maximum median response (BITC at 1:100 vol/vol) for each Or
624 across all odorants. This normalization served to adjust for the potential intrinsic differences in response
625 magnitude between the ab3A and at1 empty neuron systems²⁸.

626

627 **Behavioral tests**

628 The olfactory responses of mated, fed adult female *D. melanogaster* (Canton-S), *S. pallida*, *S.*
629 *flava*, and transgenic flies were tested using a custom-made dual-choice “Y-shaped” olfactometer⁶⁴
630 (Figure supplement 6). Flies were starved 24 hours for experiments shown in Figure 5-6. The “Y piece”
631 of the olfactometer was a propylene connector, and the arms of the “Y” were each connected to a 1-ml
632 syringe containing a piece of filter paper (6 x 50 mm) loaded with the odor or control stimuli. Charcoal-
633 filtered air was delivered to each of the two stimulus syringes using silicon tubing at 250 ml/min; thus,
634 at the base of the maze the air flow was approximately 500 ml/min. Two hours (in the case of *D.*
635 *melanogaster* and *S. pallida*) or *ca.* 20 hours before tests (in the case of *S. flava*) insects were gently
636 anesthetized under CO₂ and placed in groups of three-four in open-top and mesh-bottom cylindrical
637 release containers (20 mm long x 10 mm diameter) constructed using silicon tubing. The open top of the
638 containers was capped with a piece of cotton soaked in distilled water (in the case of *D. melanogaster*
639 and *S. pallida*) or with a piece of cotton soaked in 10% vol/vol aqueous honey solution (in the case of *S.*
640 *flava*). Before tests, each release tube was placed on ice for 45-60 seconds to slow down insect activity;

641 the cotton cap was then removed and the open-top of the tube was carefully slid into the open end of the
642 Y maze. Thus, upon being released, insects could walk upwind towards the “decision point”
643 (intersection of the short and long arms of the “Y”) and turn towards either the odor-laden or the
644 odorless arm of the maze. Although three-four insects were released at once (to increase experimental
645 efficacy), only the first choice (and the time of the choice) was recorded; a choice was considered as
646 such only if the insect walked past at least 10 mm into one of the arms, orienting upwind. The test was
647 discarded if two or more insects chose different arms of the maze within a five-second window of each
648 other. Each test lasted a maximum of five minutes, and each group of insects was used only once. Test
649 stimuli were randomly assigned to flies prepared for behavioral tests. As much as possible, insects from
650 the same cohort were tested in the same day with different odors/odorants. In the case of experiments
651 using transgenic fly lines and the progeny of crosses between them, we conducted experiments with the
652 progeny of at least 4-5 independent crosses; control and test flies were tested in parallel as much as
653 possible. Tests with each combination of fly line (or species) and stimulus were conducted in at least
654 five different days with different progeny to compensate for possible day-to-day and cohort variations.

655 In general, results from an individual test session with a given odor/odorant were discarded if
656 insects did not make a choice in more than 50% of tests (this happened in less than 5-10% of
657 experimental sessions except for *S. pallida*, which often had low activity levels), as it is the standard in
658 this type of experiment. The position of the odor and odorless arms was switched every 1-2 tests to
659 control for positional asymmetries; the mazes and odor sources were changed and replaced for
660 clean/new ones every 4 tests or 10 minutes, whichever occurred first.

661 The odor/odorant was loaded on a piece of filter paper and inserted into the 1 ml syringe
662 immediately prior to each test; control syringes had a piece of filter paper loaded with the mineral oil
663 solvent (for odorant solutions) or water (in tests apple cider vinegar). Experimental and control filter

664 papers were replaced by fresh ones every 4 tests or about 10-11 minutes, whichever came first. The
665 odorants (20 μ l of 1:100 vol/vol mineral oil solution unless noted) used in experiments were BITC
666 (Sigma-Aldrich, CAS # 592-82-5, USA) and SBITC (Sigma-Aldrich, CAS # 15585-98-5, USA), and
667 acetophenone (Sigma-Aldrich, CAS # 98-86-2, USA) in one experiment (Figure 6C). We also used
668 apple cider vinegar (40 μ l, O Organics, USA; 40 μ l of distilled water was a control stimulus in these
669 tests). For tests of host-orientation, leaves from four to six weeks old *E. sativa*, *A. thaliana*, or *S.*
670 *lycopersicum* plants, grown in an insect and insecticide/pesticide free chamber or greenhouse, were
671 excised and gently broken just before tests and placed in 5 ml syringes connected to the Y-maze; control
672 syringes had two pieces of wet tissue paper. Plant material and stimulation syringes were replaced by
673 new ones every four tests (*e.g.* after a potential maximum of 20 minutes since excision from the plant,
674 but more often after only 8-10 minutes). In all cases the Y-mazes, tubing and syringes were washed with
675 70% ethanol and allowed to air-dry before reusing. Experiments were conducted during the 2nd-5th hour
676 of the insects' photophase at 24 °C under white light (Feit electric, 100 Watts; in the case of *S. pallida*
677 and *D. melanogaster*). Green light (Sunlite green, 100 Watts) was used in the case of experiments with
678 *S. flava*, as anecdotal observations suggest that this fly species is more active under this light color, itself
679 a potentially biologically meaningful response. In all cases the total number of tests in which at least one
680 insect chooses one or the other arm of the maze is indicated in the figures for each species/fly line/odor.
681 For behavioral tests, we established “*a priori*” a minimum sample size (n=30); sample sizes for
682 experiments with *S. pallida*, which is unusually inactive, were sometimes lower but averaged n=28
683 across experimental series (Figure 5).

684 Because *S. flava* females lay eggs in leaves, generation of mutants using CRISPR-Cas9 was not
685 possible at the time of these experiments. Therefore, we conducted a gain of function tests in which *D.*
686 *melanogaster* flies expressed *Sfla* Or67b3 in the basiconic ab3A “empty neuron”, or in ab9b OSNs

687 (which express Or67b in *D. melanogaster*¹⁰²). Controls and experimental flies were tested with butyl-
688 ITC 1:1,000 vol/vol. To investigate the role of the Or67b circuit in mediating olfactory attraction, we
689 expressed UAS-Kir2.1, a genetically encoded inwardly rectifying potassium channel that by keeping
690 cells hyperpolarized prevents neuronal excitation⁶⁹, under the control of Or67b-Gal4. Experimental and
691 control fly lines were starved during 24 hours (but provided with a wet tissue paper) and tested with
692 acetophenone 1:50,000 vol/vol. To verify that previously reported behavioral responses to acetophenone
693⁶⁸ occurred under our experimental conditions, *D. melanogaster* flies (Canton-S) were also tested with
694 various concentrations of this odorant (Figure supplement 8).

695 For each odor/odorant, species, and fly line, the number of tests in which an insect made a choice
696 for one or the other arm of the Y-maze (with the criteria described above) were tested against a 50%
697 expected random distribution using two-tailed Binomial tests¹⁰³. Results were considered statistically
698 significant if $p < 0.05$. Data collection for each experimental series ended when significance was
699 achieved, or when $n=55$, regardless of the outcome. This criterion was adopted because binomial tests
700 require an untenably large sample size to evince small deviations from an expected proportion (*e.g.* 78
701 tests are required to detect a 10% deviation from the expected 50% random choice at the $p < 0.05$ level).
702 In cases where $n < 55$, we conducted a similar number of tests for control and experimental lines to
703 ensure that results are fairly comparable. Similarly, we also noted behavioral results when p-values were
704 > 0.05 but < 0.08 , because such outcomes indicate that significance ($p < 0.05$) could likely be achieved by
705 increasing sample size¹⁰¹ (although increasing sample size is often difficult for behavioral experiments).
706 For instance, a 10% deviation from the expected 50% distribution and $n=55$ yields $p=0.08$, while that
707 same deviation requires $n \geq 74$ for achieving $p < 0.05$. Thus, p-values slightly larger than 0.05 bear
708 relevant information because they are indicative of trends that might become significant if sample size
709 were increased. Statistical power was in most significant cases > 0.8 ; exceptions include cases where

710 deviations from the expected 50% distribution were relatively small (*e.g.* a significant 10% deviation
711 requires $n=188$ to achieve 0.8 statistical power).

712

713 **Data Analysis and figure generation**

714 All images and drawings are originals prepared by the authors. Figures were prepared via a
715 combination of WinEDR (v3.9.1), R Studio (v1.2.1335), Microsoft Excel (2016), Adobe Illustrator
716 (2019), ChemDraw (19.0), Python, and Geneious (10.0.9).

717

718 **Acknowledgments**

719 We are grateful to Drs. Chauda Sebastian, Dennis Mathew, John Carlson, Barry J. Dickson and
720 Bloomington Drosophila Stock Center (NIH P40OD018537) for sharing *M2-MD*, *UAS-Dmel Or67b*,
721 and *Or67d^{Gal4}*, and to Drs. Johannes Bischof and Konrad Basler for donation of the pUASTattB plasmid.
722 C.E.R. thanks Dr. Kristin Scott for support and encouragement. T.M. thanks Dr. Makoto Hiroi for
723 advice on SSR experiments. We thank members of the Whiteman and Scott Laboratories for discussions
724 and comments on the manuscript. This work was supported by the Uehara Memorial Foundation (award
725 number 201931028 to T.M.), the National Institute of General Medical Sciences of the National
726 Institutes of Health (award number R35GM119816 to N.K.W.) and the National Science Foundation
727 (award number IOS 1755188 and DEB 1601355 supporting B.G.-H.).

728

729

730

731

732 **REFERENCES**

- 733 1. Frankel, G. The raison d'être of secondary plant substances. *Science* **129**, 1466–1470 (1959).
- 734 2. Kang, K. *et al.* Analysis of *Drosophila* TRPA1 reveals an ancient origin for human chemical
735 nociception. *Nature* **464**, 597–600 (2010).
- 736 3. Lichtenstein, E. P., Strong, F. M. & Morgan, D. G. Naturally Occurring Insecticides, Identification
737 of 2-Phenylethylisothiocyanate As an Insecticide Occurring Naturally in the Edible Part of Turnips.
738 *J. Agric. Food Chem.* **10**, 30–33 (1962).
- 739 4. Berenbaum, M. R. & Zangerl, A. R. Facing the future of plant-insect interaction research: le retour
740 à la 'raison d'être'. *Plant Physiol.* **146**, 804 (2008).
- 741 5. Eckenrode, C. J. & Arn, H. Trapping cabbage maggots with plant bait and allyl isothiocyanate. *J.*
742 *Econ. Entomol.* **65**, 1343–1345 (1972).
- 743 6. Pivnick, K. A., Reed, D. W., Millar, J. G. & Underhill, E. W. Attraction of northern false chinch
744 bug *Nysius niger* (Heteroptera: Lygaeidae) to mustard oils. *Journal of Chemical Ecology* vol. 17
745 931–941 (1991).
- 746 7. Demirel, N. & Cranshaw, W. Relative attraction of color traps and plant extracts to the false chinch
747 bug *Nysius raphanus* and its parasitoid, *Phasia occidentis*, on brassica crops in colorado.
748 *Phytoparasitica* **34**, 197–203 (2006).
- 749 8. Pivnick, K. A., Jarvis, B. J. & Slater, G. P. Identification of olfactory cues used in host-plant
750 finding by diamondback moth, *Plutella xylostella* (Lepidoptera: Plutellidae). *J. Chem. Ecol.* **20**,
751 1407–1427 (1994).
- 752 9. Kergunteuil, A., Dugravot, S., Mortreuil, A., Le Ralec, A. & Cortesero, A. M. Selecting volatiles to
753 protect brassicaceous crops against the cabbage root fly, *Delia radicum*. *Entomol. Exp. Appl.* **144**,
754 69–77 (2012).

- 755 10. Liu, X.-L. *et al.* The Molecular Basis of Host Selection in a Crucifer-Specialized Moth. *Curr. Biol.*
756 **30**, 4476–4482.e5 (2020).
- 757 11. Bernays, E. & Graham, M. On the evolution of host specificity in phytophagous arthropods.
758 *Ecology* **69**, 886–892 (1988).
- 759 12. Lapoint, R. T., O’Grady, P. M. & Whiteman, N. K. Diversification and dispersal of the Hawaiian
760 Drosophilidae: the evolution of *Scaptomyza*. *Mol. Phylogenet. Evol.* **69**, 95–108 (2013).
- 761 13. Gloss, A. D. *et al.* Evolution of herbivory remodels a *Drosophila* genome. *bioRxiv* 767160 (2019)
762 doi:10.1101/767160.
- 763 14. Pelaez, J. N., Gloss, A. D., Ray, J. F. & Whiteman, N. K. Evolution and genetic basis of the plant-
764 penetrating ovipositor, a key adaptation in the transition to herbivory within the Drosophilidae.
765 *Cold Spring Harbor Laboratory* 2020.05.07.083253 (2020) doi:10.1101/2020.05.07.083253.
- 766 15. Whiteman, N. K. *et al.* Mining the plant–herbivore interface with a leafmining *Drosophila* of
767 *Arabidopsis*. *Mol. Ecol.* **20**, 995–1014 (2011).
- 768 16. Mitchell-Olds, T. *Arabidopsis thaliana* and its wild relatives: a model system for ecology and
769 evolution. *Trends Ecol. Evol.* **16**, 693–700 (2001).
- 770 17. Gloss, A. D. *et al.* Evolution in an ancient detoxification pathway is coupled with a transition to
771 herbivory in the drosophilidae. *Mol. Biol. Evol.* **31**, 2441–2456 (2014).
- 772 18. Chittenden, H. M. *The American Fur Trade of the Far West: A History of the Pioneer Trading*
773 *Posts and Early Fur Companies of the Missouri Valley and the Rocky Mountains and the Overland*
774 *Commerce with Santa Fe.* (F.P. Harper, 1902).
- 775 19. Kawahara, A. Y. *et al.* Phylogenomics reveals the evolutionary timing and pattern of butterflies and
776 moths. *Proc. Natl. Acad. Sci. U. S. A.* **116**, 22657–22663 (2019).
- 777 20. McKenna, D. D. *et al.* The evolution and genomic basis of beetle diversity. *Proc. Natl. Acad. Sci.*

- 778 *U. S. A.* **116**, 24729–24737 (2019).
- 779 21. Goldman-Huertas, B. *et al.* Evolution of herbivory in Drosophilidae linked to loss of behaviors,
780 antennal responses, odorant receptors, and ancestral diet. *Proc. Natl. Acad. Sci. U. S. A.* **112**, 3026–
781 3031 (2015).
- 782 22. Ohno, S. The Enormous Diversity in Genome Sizes of Fish as a Reflection of Nature's Extensive
783 Experiments with Gene Duplication. *Trans. Am. Fish. Soc.* **99**, 120–130 (1970).
- 784 23. Edger, P. P. *et al.* The butterfly plant arms-race escalated by gene and genome duplications. *Proc.*
785 *Natl. Acad. Sci. U. S. A.* **112**, 8362–8366 (2015).
- 786 24. Wheat, C. W. *et al.* The genetic basis of a plant–insect coevolutionary key innovation. *Proc. Natl.*
787 *Acad. Sci. U. S. A.* **104**, 20427–20431 (2007).
- 788 25. Heckel, D. G. Insect detoxification and sequestration strategies. *Annual Plant Reviews online* 77–
789 114 (2018) doi:10.1002/9781119312994.apr0507.
- 790 26. Joseph, R. M. & Carlson, J. R. *Drosophila* Chemoreceptors: A Molecular Interface Between the
791 Chemical World and the Brain. *Trends in Genetics* vol. 31 683–695 (2015).
- 792 27. Stensmyr, M. C. *et al.* A conserved dedicated olfactory circuit for detecting harmful microbes in
793 *Drosophila*. *Cell* **151**, 1345–1357 (2012).
- 794 28. Kurtovic, A., Widmer, A. & Dickson, B. J. A single class of olfactory neurons mediates
795 behavioural responses to a *Drosophila* sex pheromone. *Nature* **446**, 542–546 (2007).
- 796 29. Butenandt, A. *Über den Sexual-Lockstoff des Seidenspinners Bombyx mori: Reindarstellung und*
797 *Konstitution.* (Verlag d. Zeitschr. f. Naturforschung, 1959).
- 798 30. Sakurai, T. *et al.* Identification and functional characterization of a sex pheromone receptor in the
799 silkmoth *Bombyx mori*. *Proc. Natl. Acad. Sci. U. S. A.* **101**, 16653–16658 (2004).
- 800 31. Dweck, H. K. M. *et al.* Olfactory preference for egg laying on citrus substrates in *Drosophila*.

- 801 *Curr. Biol.* **23**, 2472–2480 (2013).
- 802 32. Dekker, T., Ibba, I., Siju, K. P., Stensmyr, M. C. & Hansson, B. S. Olfactory shifts parallel
803 superspecialism for toxic fruit in *Drosophila melanogaster* sibling, *D. sechellia*. *Curr. Biol.* **16**,
804 101–109 (2006).
- 805 33. Linz, J. *et al.* Host plant-driven sensory specialization in *Drosophila erecta*. *Proc. Biol. Sci.* **280**,
806 20130626 (2013).
- 807 34. Guo, S. & Kim, J. Molecular Evolution of *Drosophila* Odorant Receptor Genes. *Molecular Biology*
808 *and Evolution* vol. 24 1198–1207 (2007).
- 809 35. Robertson, H. M., Warr, C. G. & Carlson, J. R. Molecular evolution of the insect chemoreceptor
810 gene superfamily in *Drosophila melanogaster*. *Proc. Natl. Acad. Sci. U. S. A.* **100 Suppl 2**, 14537–
811 14542 (2003).
- 812 36. Schneiderman, A. M., Matsumoto, S. G. & Hildebrand, J. G. Trans-sexually grafted antennae
813 influence development of sexually dimorphic neurones in moth brain. *Nature* **298**, 844–846 (1982).
- 814 37. Auer, T. O. *et al.* Olfactory receptor and circuit evolution promote host specialization. *Nature*
815 (2020) doi:10.1038/s41586-020-2073-7.
- 816 38. Zhao, Z. & McBride, C. S. Correction to: Evolution of olfactory circuits in insects. *J. Comp.*
817 *Physiol. A Neuroethol. Sens. Neural Behav. Physiol.* **206**, 663 (2020).
- 818 39. Kreher, S. A., Kwon, J. Y. & Carlson, J. R. The molecular basis of odor coding in the *Drosophila*
819 larva. *Neuron* **46**, 445–456 (2005).
- 820 40. Montague, S. A., Mathew, D. & Carlson, J. R. Similar odorants elicit different behavioral and
821 physiological responses, some supersustained. *J. Neurosci.* **31**, 7891–7899 (2011).
- 822 41. Yang, Z. PAML 4: phylogenetic analysis by maximum likelihood. *Mol. Biol. Evol.* **24**, 1586–1591
823 (2007).

- 824 42. Hoare, D. J. *et al.* Modeling peripheral olfactory coding in *Drosophila* larvae. *PLoS One* **6**, e22996
825 (2011).
- 826 43. Chin, S. G., Maguire, S. E., Huoviala, P., Jefferis, G. S. X. E. & Potter, C. J. Olfactory Neurons and
827 Brain Centers Directing Oviposition Decisions in *Drosophila*. *Cell Rep.* **24**, 1667–1678 (2018).
- 828 44. Crowley-Gall, A. *et al.* Population differences in olfaction accompany host shift in *Drosophila*
829 *mojavensis*. *Proc. Biol. Sci.* **283**, (2016).
- 830 45. Hallem, E. A. & Carlson, J. R. The odor coding system of *Drosophila*. *Trends in Genetics* vol. 20
831 453–459 (2004).
- 832 46. Dobritsa, A. A., van der Goes van Naters, W., Warr, C. G., Steinbrecht, R. A. & Carlson, J. R.
833 Integrating the molecular and cellular basis of odor coding in the *Drosophila* antenna. *Neuron* **37**,
834 827–841 (2003).
- 835 47. Faucher, C. P., Hilker, M. & de Bruyne, M. Interactions of carbon dioxide and food odours in
836 *Drosophila*: olfactory hedonics and sensory neuron properties. *PLoS One* **8**, e56361 (2013).
- 837 48. Schauer, N., Zamir, D. & Fernie, A. R. Metabolic profiling of leaves and fruit of wild species
838 tomato: a survey of the *Solanum lycopersicum* complex. *J. Exp. Bot.* **56**, 297–307 (2005).
- 839 49. Fahey, J. W., Zalcman, A. T. & Talalay, P. The chemical diversity and distribution of
840 glucosinolates and isothiocyanates among plants. *Phytochemistry* **56**, 5–51 (2001).
- 841 50. Beekwilder, J. *et al.* The impact of the absence of aliphatic glucosinolates on insect herbivory in
842 *Arabidopsis*. *PLoS One* **3**, (2008).
- 843 51. Glazebrook, J. & Ausubel, F. M. Isolation of phytoalexin-deficient mutants of *Arabidopsis thaliana*
844 and characterization of their interactions with bacterial pathogens. *Proc. Natl. Acad. Sci. U. S. A.*
845 **91**, 8955–8959 (1994).
- 846 52. Sønderby, I. E. *et al.* A systems biology approach identifies a R2R3 MYB gene subfamily with

- 847 distinct and overlapping functions in regulation of aliphatic glucosinolates. *PLoS One* **2**, e1322
848 (2007).
- 849 53. Zhao, Y. *et al.* Trp-dependent auxin biosynthesis in *Arabidopsis*: involvement of cytochrome P450s
850 CYP79B2 and CYP79B3. *Genes Dev.* **16**, 3100–3112 (2002).
- 851 54. Schuhegger, R. *et al.* CYP71B15 (PAD3) catalyzes the final step in camalexin biosynthesis. *Plant*
852 *Physiol.* **141**, 1248–1254 (2006).
- 853 55. Münch, D. & Galizia, C. G. DoOR 2.0--Comprehensive Mapping of *Drosophila melanogaster*
854 Odorant Responses. *Sci. Rep.* **6**, 21841 (2016).
- 855 56. Rasmann, S. *et al.* Recruitment of entomopathogenic nematodes by insect-damaged maize roots.
856 *Nature* vol. 434 732–737 (2005).
- 857 57. Degen, T., Dillmann, C., Marion-Poll, F. & Turlings, T. C. J. High genetic variability of herbivore-
858 induced volatile emission within a broad range of maize inbred lines. *Plant Physiol.* **135**, 1928–
859 1938 (2004).
- 860 58. Sultana, T., Savage, G. P., McNeil, D. L., Porter, N. G. & Clark, B. Comparison of flavour
861 compounds in wasabi and horseradish. *J. Food Agric. Environ* **1**, 117–121 (2003).
- 862 59. Xue, Y.-L. *et al.* Multivariate analyses of the volatile components in fresh and dried turnip
863 (*Brassica rapa* L.) chips via HS-SPME-GC-MS. *J. Food Sci. Technol.* **57**, 3390–3399 (2020).
- 864 60. Ishii, G., Saijo, R. & Mizutani, J. A quantitative determination of 4-methylthio-3-butenyl
865 glucosinolate in daikon (*Raphanus sativus* L.) roots by gas liquid chromatography. *J. Japan. Soc.*
866 *Hortic. Sci.* **58**, 339–344 (1989).
- 867 61. Richardson, B. Identification and characterization of potent odorants in selected beet root (*Beta*
868 *vulgaris*) products. (2013).
- 869 62. Allmann, S. *et al.* Feeding-induced rearrangement of green leaf volatiles reduces moth oviposition.

- 870 *eLife* vol. 2 (2013).
- 871 63. Syed, T. H., Famiglietti, J. S., Chambers, D. P., Willis, J. K. & Hilburn, K. Satellite-based global-
872 ocean mass balance estimates of interannual variability and emerging trends in continental
873 freshwater discharge. *Proc. Natl. Acad. Sci. U. S. A.* **107**, 17916–17921 (2010).
- 874 64. Reisenman, C. E., Lee, Y., Gregory, T. & Guerenstein, P. G. Effects of starvation on the olfactory
875 responses of the blood-sucking bug *Rhodnius prolixus*. *J. Insect Physiol.* **59**, 717–721 (2013).
- 876 65. Aurand, L. W., Singleton, J. A., Bell, T. A. & Etchells, J. L. Volatile Components in the Vapors of
877 Natural and Distilled Vinegars. *J. Food Sci.* **31**, 172–177 (1966).
- 878 66. Cousin, F. J. *et al.* Microorganisms in Fermented Apple Beverages: Current Knowledge and Future
879 Directions. *Microorganisms* **5**, (2017).
- 880 67. Mansourian, S. *et al.* Wild African *Drosophila melanogaster* Are Seasonal Specialists on Marula
881 Fruit. *Curr. Biol.* **28**, 3960–3968.e3 (2018).
- 882 68. Strutz, A. *et al.* Decoding odor quality and intensity in the *Drosophila* brain. *Elife* **3**, e04147
883 (2014).
- 884 69. Baines, R. A., Uhler, J. P., Thompson, A., Sweeney, S. T. & Bate, M. Altered electrical properties
885 in *Drosophila* neurons developing without synaptic transmission. *J. Neurosci.* **21**, 1523–1531
886 (2001).
- 887 70. Jaenike, J. Host specialization in phytophagous insects. *Annu. Rev. Ecol. Syst.* **21**, 243–273 (1990).
- 888 71. Galizia, C. & Sachse, S. Odor Coding in Insects. *Frontiers in Neuroscience* 35–70 (2009)
889 doi:10.1201/9781420071993-c2.
- 890 72. Heidel-Fischer, H. M. *et al.* An Insect Counteradaptation against Host Plant Defenses Evolved
891 through Concerted Neofunctionalization. *Mol. Biol. Evol.* **36**, 930–941 (2019).
- 892 73. He, X. & Zhang, J. Rapid subfunctionalization accompanied by prolonged and substantial

- 893 neofunctionalization in duplicate gene evolution. *Genetics* **169**, 1157–1164 (2005).
- 894 74. Assis, R. & Bachtrog, D. Neofunctionalization of young duplicate genes in *Drosophila*. *Proc. Natl.*
895 *Acad. Sci. U. S. A.* **110**, 17409–17414 (2013).
- 896 75. Prieto-Godino, L. L. *et al.* Evolution of Acid-Sensing Olfactory Circuits in Drosophilids. *Neuron*
897 **93**, 661–676.e6 (2017).
- 898 76. Bruce, T. J. A. & Pickett, J. A. Perception of plant volatile blends by herbivorous insects--finding
899 the right mix. *Phytochemistry* **72**, 1605–1611 (2011).
- 900 77. Chaverra-Rodriguez, D. *et al.* Targeted delivery of CRISPR-Cas9 ribonucleoprotein into arthropod
901 ovaries for heritable germline gene editing. *Nat. Commun.* **9**, 3008 (2018).
- 902 78. Macpherson, L. J. *et al.* Noxious compounds activate TRPA1 ion channels through covalent
903 modification of cysteines. *Nature* **445**, 541–545 (2007).
- 904 79. Hinman, A., Chuang, H.-H., Bautista, D. M. & Julius, D. TRP channel activation by reversible
905 covalent modification. *Proc. Natl. Acad. Sci. U. S. A.* **103**, 19564–19568 (2006).
- 906 80. Piersanti, S., Reborá, M., Ederli, L., Pasqualini, S. & Salerno, G. Role of chemical cues in cabbage
907 stink bug host plant selection. *J. Insect Physiol.* **120**, 103994 (2020).
- 908 81. Renwick, J. A. A., Haribal, M., Gouinguéné, S. & Städler, E. Isothiocyanates stimulating
909 oviposition by the diamondback moth, *Plutella xylostella*. *J. Chem. Ecol.* **32**, 755–766 (2006).
- 910 82. Kim, B. Y. *et al.* Highly contiguous assemblies of 101 drosophilid genomes. *Elife* **10**, (2021).
- 911 83. Thurmond, J. *et al.* FlyBase 2.0: the next generation. *Nucleic Acids Res.* **47**, D759–D765 (2019).
- 912 84. Katoh, K. MAFFT: a novel method for rapid multiple sequence alignment based on fast Fourier
913 transform. *Nucleic Acids Research* vol. 30 3059–3066 (2002).
- 914 85. Nguyen, L.-T., Schmidt, H. A., von Haeseler, A. & Minh, B. Q. IQ-TREE: A Fast and Effective
915 Stochastic Algorithm for Estimating Maximum-Likelihood Phylogenies. *Molecular Biology and*

- 916 *Evolution* vol. 32 268–274 (2015).
- 917 86. Stamatakis, A. RAxML version 8: a tool for phylogenetic analysis and post-analysis of large
918 phylogenies. *Bioinformatics* vol. 30 1312–1313 (2014).
- 919 87. Kim, B. Y. *et al.* Highly contiguous assemblies of 101 drosophilid genomes. *Cold Spring Harbor*
920 *Laboratory* 2020.12.14.422775 (2020) doi:10.1101/2020.12.14.422775.
- 921 88. Katoh, T., Izumitani, H. F., Yamashita, S. & Watada, M. Multiple origins of Hawaiian
922 drosophilids: phylogeography of *Scaptomyza hardy* (Diptera: Drosophilidae). *Entomol. Sci.* **20**, 33–
923 44 (2017).
- 924 89. Lanfear, R., Frandsen, P. B., Wright, A. M., Senfeld, T. & Calcott, B. PartitionFinder 2: New
925 Methods for Selecting Partitioned Models of Evolution for Molecular and Morphological
926 Phylogenetic Analyses. *Mol. Biol. Evol.* **34**, 772–773 (2017).
- 927 90. Bouckaert, R. *et al.* BEAST 2.5: An advanced software platform for Bayesian evolutionary
928 analysis. *PLoS Comput. Biol.* **15**, e1006650 (2019).
- 929 91. Swofford, D. L. PAUP: phylogenetic analysis using parsimony, version 4.0 b10. (2002).
- 930 92. Ronquist, F. *et al.* MrBayes 3.2: efficient Bayesian phylogenetic inference and model choice across
931 a large model space. *Syst. Biol.* **61**, 539–542 (2012).
- 932 93. Guindon, S. *et al.* New Algorithms and Methods to Estimate Maximum-Likelihood Phylogenies:
933 Assessing the Performance of PhyML 3.0. *Systematic Biology* vol. 59 307–321 (2010).
- 934 94. Benjamini, Y. & Hochberg, Y. Controlling the False Discovery Rate: A Practical and Powerful
935 Approach to Multiple Testing. *Journal of the Royal Statistical Society: Series B (Methodological)*
936 vol. 57 289–300 (1995).
- 937 95. Gross, L. A., Baird, G. S., Hoffman, R. C., Baldrige, K. K. & Tsien, R. Y. The structure of the
938 chromophore within DsRed, a red fluorescent protein from coral. *Proc. Natl. Acad. Sci. U. S. A.* **97**,

- 939 11990–11995 (2000).
- 940 96. Bischof, J., Maeda, R. K., Hediger, M., Karch, F. & Basler, K. An optimized transgenesis system
941 for *Drosophila* using germ-line-specific ϕ C31 integrases. *Proc. Natl. Acad. Sci. U. S. A.* **104**, 3312–
942 3317 (2007).
- 943 97. Hallem, E. A. & Carlson, J. R. Coding of Odors by a Receptor Repertoire. *Cell* vol. 125 143–160
944 (2006).
- 945 98. Gonzalez, F., Witzgall, P. & Walker, W. B. Protocol for Heterologous Expression of Insect
946 Odourant Receptors in *Drosophila*. *Front. Ecol. Evol.* **4**, 189 (2016).
- 947 99. Stensmyr, M. C., Giordano, E., Balloi, A., Angioy, A.-M. & Hansson, B. S. Novel natural ligands
948 for *Drosophila* olfactory receptor neurones. *J. Exp. Biol.* **206**, 715–724 (2003).
- 949 100. Olsson, S. B., Linn, C. E., Jr & Roelofs, W. L. The chemosensory basis for behavioral divergence
950 involved in sympatric host shifts. I. Characterizing olfactory receptor neuron classes responding to
951 key host volatiles. *J. Comp. Physiol. A Neuroethol. Sens. Neural Behav. Physiol.* **192**, 279–288
952 (2006).
- 953 101. Makin, T. R. & de Xivry, J.-J. O. Science forum: Ten common statistical mistakes to watch out for
954 when writing or reviewing a manuscript. *Elife* **8**, e48175 (2019).
- 955 102. Couto, A., Alenius, M. & Dickson, B. J. Molecular, anatomical, and functional organization of the
956 *Drosophila* olfactory system. *Curr. Biol.* **15**, 1535–1547 (2005).
- 957 103. Zar, J. H. *Biostatistical Analysis*. (Prentice Hall, 1999).
- 958 104. Willmore, B. & Tolhurst, D. J. Characterizing the sparseness of neural codes. *Network* **12**, 255–270
959 (2001).
- 960 105. Dekker, T., Ibba, I., Siju, K. P., Stensmyr, M. C. & Hansson, B. S. Olfactory shifts parallel
961 superspecialism for toxic fruit in *Drosophila melanogaster* sibling, *D. sechellia*. *Curr. Biol.* **16**,

962 101–109 (2006).

963 106. Keeseey, I. *et al.* Evolution of a pest: towards the complete neuroethology of *Drosophila suzukii* and
964 the subgenus *Sophophora*. *BioRxiv* (2019).

965 107. Prieto-Godino, L. L. *et al.* Olfactory receptor pseudo-pseudogenes. *Nature* vol. 539 93–97 (2016).

966

967 **FIGURE CAPTIONS**

968 **Figure 1 Maximum likelihood (ML) phylogeny of *Or67b* in Drosophilidae.**

969 **(A)** Time-calibrated Bayesian chronogram of *Scaptomyza* and *Drosophila* spp. inferred from nine
970 protein coding and two ribosomal genes. Source species for the *Or67b* coding sequences crossed into the
971 empty neuron system are indicated with fly pictograms. Bars indicate 95% highest posterior density
972 (HPD) age estimates in millions of years ago. Tree topology labeled as follows: Posterior Probability
973 (PP):ML BS:Parsimony BS on branches. Scale bar proportional to MYA. **(B)** ML phylogeny
974 reconstructed based on the coding sequence of *Or67b* orthologs from twelve *Drosophila* species, *S.*
975 *pallida*, *S. hsui*, *S. graminum*, and *S. flava*. All bootstrap supports for the nodes are >80% and all
976 posterior probabilities were >0.95 for the MrBayes tree. Branches with significant support (FDR p-value
977 < 0.05) for d_N/d_S values different from the background rate are indicated with colored branch labels
978 (blue where the foreground rate is less than the background, and red/enlarged fonts where d_N/d_S is
979 greater than the background). Only *S. flava* and *D. mojavensis* branches have significantly elevated d_N/d_S
980 according to branch model tests. *S. flava*, *S. pallida* and *D. melanogaster* labeled identically to (A).
981 Scale bar units are substitutions per site.

982

983

984

985 **Figure 2 Responses of homologs Or67bs from *D. melanogaster*, *S. pallida*, and *S. flava* expressed in**
986 **the *D. melanogaster* empty neuron systems to stimulation with natural odor blends.**

987 (A) Schematic representation of the single sensillum recording (SSR) using two “empty neuron
988 systems”. Or67b proteins (*X_Or67b*, where *X* refers to the fly species) were expressed in a *D.*
989 *melanogaster* mutant that lacks its endogenous *Or22a* in ab3A (antennal basiconic 3A) OSNs⁹⁷, or
990 *Or67d* in at1 (antennal trichoid 1) OSNs²⁸. Note that the at1 empty neuron system was used only for
991 expression of *Sfla* Or67b2, as this Or was not functional in the ab3A empty neuron system. In the
992 antennal basiconic empty neuron system (left) the sensilla houses the A neuron (which expresses one of
993 the Or67b proteins) and the native intact B neuron. The A neuron has larger amplitude spikes than the B
994 neuron, allowing separation of spikes originating from either of them. The antennal trichoid empty
995 neuron system houses a single OSN expressing *Sfla* Or67b2 (see also Figure supplement 3). Calibration
996 bars: 10 mV throughout all figures unless otherwise noted. (B) Representative electrophysiological
997 SSRs obtained from the targeted sensilla of flies expressing Or67b in OSNs in response to stimulation
998 with apple cider vinegar, wild-type Col-0 *Arabidopsis thaliana*, and *PAD3* and quadruple aliphatic and
999 indolic glucosinolate knockout (GKO; *CYP79B2*, *CYP79B3*, *MYB28*, *MYB29*) *A. thaliana* mutant lines.
1000 Although all three *A. thaliana* genotypes have the same genetic background⁵⁰⁻⁵¹, *PAD3* plants are a
1001 more appropriate control for GKO than Col-0, since *PAD3* is deficient (as is GKO) in the production of
1002 camalexin but not aliphatic or indolic glucosinolates. The bars above records indicate the onset and
1003 duration (1 sec) of the stimulation throughout all figures unless otherwise noted. (C) Responses (net
1004 number of spikes/second, control-subtracted, n=6-9 obtained from 2-4 animals) evoked by stimulation
1005 with apple cider vinegar, mustard leaf odors (arugula and *A. thaliana*), mustard root odors (wasabi,
1006 horseradish, turnip and daikon), non-mustard leaf odors (tomato), and non-mustard root odors (beet,
1007 control). The outer edges of the horizontal bars represent the 25% and 75% quartiles, the vertical line

1008 inside the bars represents the median, and the whiskers represent 10% and 90% quartiles; each dot
1009 represents an individual response. Asterisks indicate significant differences between the control-
1010 subtracted net number of spikes and a threshold median value (10 spikes/second), as explained in
1011 material and methods (one-sample signed rank tests; * $p < 0.05$, ** $p < 0.01$). Neurons expressing *Dmel*
1012 *Or67b* and *Spal Or67b*, but not those expressing any of the *S. flava Or67b* paralogs, responded to
1013 stimulation with apple cider vinegar. Conversely, only neurons expressing *S. flava Or67b* paralogs
1014 responded to arugula odors (which bear ITCs). *Dmel Or67b* responded to all *A. thaliana* genotypes,
1015 while *Sfla Or67b1-2* responded only to ITC-bearing *A. thaliana*, indicating that the presence of ITCs
1016 within plants is necessary to evoke responses from these two *S. flava* paralogs. Stimulation with wasabi
1017 root odors evoked responses from all *Sfla Or67b* paralogs but not from the *Dmel* or the *Spal* paralogs.

1018

1019 **Figure 3 Responses of homologs Or67bs from *D. melanogaster*, *S. pallida* and *S. flava* expressed in**
1020 **the *D. melanogaster* empty neuron systems to stimulation with single odorants.**

1021 Experiments were conducted and analyzed as in Figure 2. As before, the at1 empty neuron system was
1022 only used for expressing *Sfla Or67b2*. (A) Representative electrophysiological recordings obtained from
1023 the targeted sensilla of flies expressing *Or67b* genes in the empty neuron in response to stimulation with
1024 acetophenone and BITC at 1:100 vol/vol. (B) Responses evoked by stimulation with single odorants
1025 (tested at 1:100 vol/vol) categorized as follows: *Dmel Or67b* activators (Database of Odor Responses⁵⁵;
1026 blue), green leaf volatiles (GLVs; gray), ITCs (green), benzyl thiocyanate (yellow), nitrile (pink), and
1027 TrpA1 activators (purple). OSNs expressing any of the *Sfla Or67b* paralogs respond strongly and
1028 selectively to ITCs. Note that OSNs expressing any of the *S. flava* paralogs do not respond to benzyl
1029 thiocyanate stimulation (yellow bars), indicating that the presence of the ITC functional group (-
1030 N=C=S) is necessary for evoking responses from these paralogs. *Spal Or67b* and *Dmel Or67b* have

1031 similar odor-response profiles, responding mostly to stimulation with *D. melanogaster* activators and
1032 GLVs (*p<0.05, **p<0.01, one-sample signed rank tests performed as explained in the caption to Figure
1033 2). Most odorants were diluted in mineral oil but a few needed to be prepared in other solvents (see
1034 material and methods); spikes count in response to control solvent applied in each case were subtracted
1035 from odorant-evoked responses. (C) Tuning curves for each Or67b, showing the distribution of median
1036 responses to the 42 odorants tested (color-coded as in A). The odorants are displayed along the
1037 horizontal axis according to the net responses they elicit from each Or. The odorants (numbers) eliciting
1038 the strongest responses for each Or are located at the center of the distribution and weaker activators are
1039 distributed along the edges. Note that the strongest responses (center of the distribution) from *Dmel*
1040 Or67b and *Spal* Or67b are evoked by *D. melanogaster* activators and GLVs (blue and gray bars), while
1041 the strongest responses from all *Sfla* Or67b paralogs are evoked by ITCs (green bars). The tuning
1042 breadth of each Or is quantified by the kurtosis value (k) of the distribution ¹⁰⁴, with higher values
1043 indicating narrower odor-response profiles. The chemical structure of the top seven *Sfla* Or67b3
1044 activators, as well as AITC, citronellal, acetophenone, *cis*-3-hexenyl butyrate and benzyl thiocyanate
1045 (BTC) are shown at the bottom.

1046

1047 **Figure 4 *Sfla* Or67b1-3 have distinct ITC selectivity.**

1048 (A) Dose responses of *Sfla* Or67b1, *Sfla* Or67b2 and *Sfla* Or67b3 (abbreviated as b1, b2 and b3) to
1049 stimulation with increasing concentrations (vol/vol) of eight different ITCs (categorized according to
1050 molecular structure, top boxes; odorant abbreviations are as in Figure 3). As before, the at1 empty
1051 neuron system was only used for expressing *Sfla* Or67b2. Data represent the control-subtracted net
1052 number of spikes (average ± SE; n=6-8, obtained from 2-3 animals). (B) Heatmap of dose-responses
1053 (median, color-coded) from the three *Sfla* paralog normalized (to allow comparisons across paralogs) by

1054 each paralog's median response to 1:100 vol/vol of BITC (the strongest ITC activator across all
1055 paralogs). Asterisks indicate significant differences as explained in Materials and Methods (One-sample
1056 signed rank tests; * $p < 0.05$; ** $p < 0.01$). The strongest responses were evoked by the highest ITC
1057 concentrations, with many compounds evoking responses from all paralogs, particularly in the case of
1058 *Sfla* Or67b1 and b3; the number of stimuli that evoked responses decreased with decreasing odorant
1059 concentration.

1060

1061 **Figure 5 Olfactory behavioral responses of *S. flava* and its microbe-feeding relatives *S. pallida* and**
1062 ***D. melanogaster* to ecologically related odors and ITCs.**

1063 **(A)** Schematic representation of the dual choice y-maze used to test the olfactory responses of flies (see
1064 details in Figure supplement 6, and materials and methods). One arm of the maze offered constant
1065 odor/odorant airflow (apple cider vinegar, arugula, tomato or single ITC compounds at 1:100 vol/vol),
1066 while the control arm offered a constant odorless airflow (controls: water for odors, and mineral oil for
1067 single odorants). In each test a group of non-starved flies ($n=3-4$) was released at the base of the maze
1068 and allowed to choose between the two arms of the maze. Each test (maximum duration=5 min) ended
1069 when the first insect (out of all released) made a choice. **(B)** Olfactory behavioral responses of *D.*
1070 *melanogaster*, *S. pallida* and *S. flava* to apple cider vinegar odors and VOCs from leaves of arugula and
1071 tomato plants. Data represent the percentage of tests in which animals choose the odorous or odorless
1072 (*i.e.* control: water in the case of apple cider vinegar, a piece of tissue paper in the case of plant leaves)
1073 arms of the maze; numbers between parentheses indicate the number of tests with choices for one or the
1074 other arm. For each fly species and odor/odorant compound, data was analyzed using two-tailed
1075 Binomial tests (** $p < 0.01$, **** $p < 0.001$, ***** $p < 0.0001$). *S. flava* was attracted to mustard (arugula)
1076 VOCs but not to non-mustard (tomato) VOCs; flies tended to avoid apple cider vinegar odors although

1077 differences were not significant ($p=0.054$); *D. melanogaster* was strongly attracted to apple cider
1078 vinegar but not to arugula or tomato leaf VOCs; *S. pallida* was only attracted to tomato leaf VOCs. **(C)**
1079 Olfactory behavioral responses of flies from the three species to single ITC compounds (1:100 vol/vol in
1080 mineral oil loaded in filter paper); the control arm of the olfactometer offered mineral oil loaded in filter
1081 paper. Assays were conducted as described in **B**. *S. flava* was strongly attracted to both ITC compounds
1082 tested, *S. pallida* was strongly repelled by BITC, and *D. melanogaster* was indifferent to either ITC.

1083

1084 **Figure 6 Ectopic expression of *Sfla* Or67b3 in Or22a OSNs or Or67b OSNs conferred behavioral**
1085 **responses to BITC in *D. melanogaster*.**

1086 **(A)** Behavioral responses of *D. melanogaster* flies expressing *Dmel* Or67b or *Sfla* Or67b3 in Or22a
1087 OSNs lacking its cognate olfactory receptor in dual-choice assays (BITC 1:1,000 vol/vol vs. mineral oil
1088 control). Experiments were conducted and analyzed as explained in the caption to Figure 5. The two
1089 parental control flies (first two groups) and flies expressing *Dmel* Or67b, as expected, were not attracted
1090 neither repelled by BITC (Binomial tests, $p>0.05$ in all cases). In contrast, flies expressing *Sfla* Or67b3
1091 were attracted to the odorant (* $p<0.05$). These results show that ITCs can evoke olfactory behavioral
1092 responses when *Sfla* Or67b3 is expressed in an olfactory circuit that governs attraction. **(B)** Same as **A**,
1093 but flies expressed *Dmel* Or67b or *Sfla* Or67b3 in Or67b OSNs (note that flies have the endogenous
1094 Or67b expressed in OSNs, in addition to the transgene). As in **A**, only flies carrying the *S. flava*
1095 transgene were attracted to BITC (* $p<0.05$). **(C)** Behavioral responses of *D. melanogaster* flies
1096 expressing a silencer of synaptic activity (Kir2.1) in Or67b OSNs, along with the responses of the two
1097 parental control lines (transgenes indicated to the left). One arm of the maze offered acetophenone
1098 (1:50,000 vol/vol), a strong *Dmel* Or67b activator⁵⁵ (Figure 3), while the other arm had mineral oil.
1099 Experiments were conducted as explained in the caption to Figure 5, but flies were starved 24 hours

1100 previous to testing. As observed for wild-type flies (see Figure supplement 8 and ref. ⁶⁸), genetic control
1101 flies showed a trend ($0.05 < p < 0.08$) for attraction towards low concentrations of acetophenone, while
1102 flies with Or67b OSNs silenced lost attraction and were instead repelled by the odorant (as wild-type
1103 flies tested with higher concentrations of acetophenone; see Figure supplement 8 and ref. ⁶⁸). All these
1104 findings along with previous reports ⁴⁴ suggest that the ancestral Or67b circuit mediates olfactory
1105 attraction.

1106

1107 **Figure 7 A model for the evolution of *Or67b* and comparison with the known evolution of other Or**
1108 **orthologs in drosophilid flies.**

1109 **(A)** Model for the evolution of *Scaptomyza Or67b*. The evolution of this Or begins with a shift in the
1110 ligand specificity of an ancestral Or67b (a) tuned to *Dmel* activators, GLVs, and ITCs
1111 (neofunctionalization, b). Subsequent gene triplication of *Sfla Or67b* gave rise to two additional
1112 paralogous *Or67b* genes (*Sfla Or67b1*, *Sfla Or67b2*, and *Sfla Or67b3*; c), each of them having different
1113 but overlapping ITC odorant-receptive ranges (Figures 3 and 4). **(B)** Evolution of drosophilid orthologs
1114 with known ligand specificities (Or22a, Ir75a, Ir75b, top; and Or67b, bottom). The Or22a orthologs
1115 from *D. melanogaster* (*Dmel Or22a*), *D. sechellia* (*Dsec Or22a*), *D. erecta* (*Der Or22a*), and *D. suzukii*
1116 (*Dsuz Or22a*) are all strongly activated by species-specific host-derived esters (compounds 1-4; top left;
1117 ^{33,67,105-106}). The Ir75a orthologs from *D. melanogaster* (*Dmel Ir75a*), and *D. sechellia* (*Dsec Ir75a*) are
1118 strongly activated respectively by the acid compounds 5 and 6 ⁷⁵. Similarly, the Ir75b orthologs from *D.*
1119 *melanogaster* (*Dmel Ir75b*), and *D. sechellia* (*Dsec Ir75b*) are respectively activated by the acids 7 and 8
1120 (top right; ¹⁰⁷). *Dmel Or67b* and *Spal Or67b* are strongly activated respectively by acetophenone and *cis*-
1121 3-hexenyl butyrate (compounds 9 and 10), while *Sfla Or67b* paralogs are activated by ITCs only
1122 (bottom, paralog-specific activation by compounds 11-13). Note that Or22a, Ir75a and Ir75b orthologs

1123 are all divergent but activated by ligands belonging to a single chemical class (whether esters or acids).
1124 On the other hand, the ligands of orthologs Or67b from *Dmel* and *Spal* are responsive to a variety of
1125 chemical classes which include alcohols, aldehydes and ketones, whereas *Sfla* Or67b orthologs are
1126 responsive to ITCs, an entirely different compound chemical class.

1127

1128 **Figure supplement 1 Maximum likelihood (ML) phylogeny of *Ors* in Drosophilidae.**

1129 ML phylogeny reconstructed from protein translations of the *Ors* found in *S. flava*, *D. melanogaster*, *D.*
1130 *grimshawi*, *D. virilis* and *D. mojavensis* genomes. Line width of branches are proportional to bootstrap
1131 support. Green branches indicate *Scaptomyza Ors*. Enlarged gene names in bold include branches with
1132 estimated $d_N/d_S > 1$. Scale bar units are substitutions per site.

1133

1134 **Figure supplement 2 Or67b protein alignment and micro-syntenic patterns of scaffolds from *S.***
1135 ***flava*, *S. pallida*, and *D. melanogaster*.**

1136 **(A)** Alignments of Or67b proteins. Note that orthologs and paralogs share a large number of amino acids
1137 (black squares). Darker colors illustrate higher degrees of sequence similarity, and lighter colors denote
1138 residues with high variability in sequence across paralogs and orthologs. Also shown are each of the
1139 seven predicted transmembrane domains (TM1-7). **(B)** Micro-syntenic patterns of Or67b scaffolds. Five
1140 genes up and downstream of each *S. flava Or67b* ortholog are shown. We determined that there was
1141 only one copy of *Or67b* in both *S. pallida* and *D. melanogaster*. Note that in both *S. pallida* and *D.*
1142 *melanogaster*, many of the pGOIs are still present and syntenic with those in *S. flava*, suggesting that the
1143 absence of the other *Or67b* orthologs is not a consequence of mis-assembly but a *bona fide* absence.

1144

1145 **Figure supplement 3 Or22a and Or67b are not expressed in the ab3A and the at1 empty neuron**
1146 **systems.**

1147 **(A)** Recordings from ab3 sensilla in empty neuron mutants (left) and wild-type flies (right).
1148 Representative electrophysiological traces confirming that in the “empty” ab3A neuron mutant fly line
1149 only the B neuron, which has smaller amplitude spikes (see also Fig. 2A), is present. As expected, the B
1150 neuron responds to stimulation with 2-heptanone 1:10,000 vol/vol (mediated by its endogenous *Or85b*,
1151 top), similar to wild-type flies (right). **(B)** In the ab3A “empty” neuron mutant, the lack of *Or22a*
1152 expression in the A neuron was verified by the lack of spiking upon stimulation with ethyl hexanoate
1153 1:100 vol/vol (left). In wild-type flies (Canton-S), as expected, the A neuron (large spikes) respond
1154 strongly to stimulation with ethyl hexanoate. The bottom part of the panel shows the population
1155 responses of mutant (left) and wild-type flies (right). Data represents the net number of spikes in
1156 response to stimulation (n= 6-7, obtained from 3 females, dots denote individual data points; boxes
1157 represent the 25 and 75% quartiles, whiskers represent the 10 and 90% quartiles, and the vertical line
1158 inside the boxes indicate the median). Differences between the responses of flies stimulated with the
1159 odorant and the control solvent were statistically different in the case of wild-type flies (right, * p<0.05,
1160 Wilcoxon-matched pairs test) but not in the case of flies lacking Or22a (left, p>0.05). **(C)** Similarly, lack
1161 of Or67d expression in the at1 neuron in the *Or67d^{GAL4}* fly line (“empty at1 neuron” mutant) was
1162 verified by the lack of responses to 11-*cis* vaccenyl acetate 1:100 vol/vol (left; ethanol was used as the
1163 solvent control). The top shows representative electrophysiological recordings and the bottom the
1164 population response (data obtained and represented as explained in A). In wild-type flies, at1 neurons
1165 respond strongly to stimulation with this compound (right, * p<0.05).

1166

1167 **Figure supplement 4 Principal component analysis (PCA) of median responses from the three *S.***
1168 ***flava* paralogs**

1169 Responses of Or67b paralogs in odor space, generated by PCA of median net spiking responses (control-
1170 subtracted) from the three *S. flava* paralogs to eight ITCs tested at 1:100 (red circles), 1:1,000 (green
1171 triangles), and 1:10,000 vol/vol (blue rectangles). The axes display the two first principal components
1172 (PC1 and PC2) which respectively explain 75% and 17% of the variance.

1173
1174 **Figure supplement 5 Antennal OSNs respond to ITCs in *S. flava*.**

1175 **(A)** Representative electrophysiological recordings obtained from antennal *S. flava* OSN housed in
1176 basiconic-like (top) and trichoid-like (bottom) sensilla in response to stimulation with BITC 1:1,000
1177 vol/vol and the mineral oil solvent control. In both cases, the OSNs with smaller spike amplitude (“B”
1178 neurons) were strongly activated by BITC. **(B)** Responses of *S. flava* individual antennal basiconic-like
1179 and trichoid-like OSNs (net number of spikes, control-subtracted; n=36; 3 individuals in each case) in
1180 response to BITC 1:1,000 vol/vol. Most basiconic and trichoid OSNs (81%) showed little or no response
1181 (median= -10 to 12 net spikes /second), but 19% showed strong responses (range: 74 to 252 and 65 to
1182 200 spikes/second for basiconic and trichoid sensilla, respectively). These results indicate that at least
1183 some OSNs are responsive to ITCs in the antenna of *S. flava*, in agreement with the finding that at least
1184 the paralogs of Or67b are tuned to these compounds in this fly species. **(C)** Schematic distribution of
1185 ITC sensitive OSNs in basiconic-like and trichoid-like sensilla on the antennae. These sensilla
1186 distributed proximally and distally (inside of the broken red and blue lines) respectively on the ventral
1187 side of antennae.

1188

1189 **Figure supplement 6 Detailed schematic representation of the device used to test olfactory**
1190 **behavioral responses.**

1191 The responses of insects were tested using a dual-choice “Y-shaped” olfactometer modified from one
1192 previously published *e.g.* ⁶⁴. The “Y” part of the maze was a propylene connector; the open ends of the
1193 arms of the connector were each connected to a 1 or a 5 ml plastic syringe containing the odor/odorant
1194 stimulus or the control stimulus. Single odorants (or the solvent control) were loaded in a piece of filter
1195 paper which was placed in 1 ml syringes; plant leaves (or wet tissue paper as a control) were placed in 5-
1196 ml syringes. Charcoal-filtered air was delivered to the maze and adjusted to 0.5 liters per minute (LPM)
1197 using a flowmeter; thus, odor airflow in each arm was 0.25 LPM, and at the base of the maze again 0.5
1198 LPM. Three-four insects were placed in individual open-top releasing containers 2 hours before
1199 experiments with a piece of tissue paper soaked in distilled water (in the case of *D. melanogaster*) or ca.
1200 20 hours with a cotton piece soaked in honey water solution (in the case of *S. flava*). For experiments in
1201 Figure 6C, transgenic flies were placed in individual releasing containers with a piece of tissue paper
1202 embedded in water 24 hours before experiments. Before each test, the release container was placed
1203 during 45-60 seconds in ice to slow down insect activity. Each test started when the open-top of the
1204 insect container was carefully slid into the open end of the long arm of the “Y”. Thus, upon being
1205 released, insects could walk upwind towards the “decision point” (intersection of the short and long
1206 arms of the “Y”) and turn towards either the odor-laden or the odorless arm of the maze. A choice was
1207 considered as such only if the insect walked past at least 1 cm into the arm, orienting upwind. Although
1208 3-4 insects were released in each test (to increase the possibility that at least one insect made a choice),
1209 only the first choice (control arm or odorous arm) was recorded. If a second insect made a choice for the
1210 other arm within 5-7 seconds of the first insect, the test was discarded. Each test lasted a maximum of
1211 five minutes, and each group of insects was used only once. The position of the control and the test arms

1212 was switched every one or two tests to control for positional asymmetries. The whole device was
1213 illuminated with white light or green light (in the case of tests with *S. flava*).

1214

1215 **Figure supplement 7 Olfactory behavioral responses of *S. flava* and its microbe-feeding relatives *S.***
1216 ***pallida* and *D. melanogaster* to *Arabidopsis*.**

1217 A dual choice y-maze was used to quantify olfactory behavioral responses of *D. melanogaster*, *S.*
1218 *pallida* and *S. flava* to *PAD3* and GKO *A. thaliana* mutants as described in Figure 5. One arm of the
1219 maze offered constant *A. thaliana* odor airflow, while the control arm offered a constant odorless
1220 humidified airflow. Data was analyzed using two-tailed Binomial tests (* $p < 0.05$, ** $p < 0.01$). *S. flava*
1221 and *D. melanogaster*, but not *S. pallida*, were attracted to leaf VOCs from both *A. thaliana* mutant lines.
1222 In this experiment only GKO and *PAD3* plants were used because as explained before, the *PAD3*
1223 genotype is a better control for GKO plants than Col-0.

1224

1225 **Figure supplement 8 Concentration-dependent behavioral responses of wild-type *D. melanogaster***
1226 **to acetophenone**

1227 Behavioral responses of (strain: Canton-S) flies tested with two concentrations of acetophenone. One
1228 arm of the maze offered either acetophenone at 1:10,000 or 1:100 vol/vol, while the other arm had
1229 mineral oil. Flies were attracted to the lower concentration but repelled by the higher concentration
1230 (Binomial tests, * $p < 0.05$; ** $p < 0.01$).

1231

1232

1233

1234 **SOURCE DATA CAPTION**

1235 **Source data *Or67bs* are expressed in *Scaptomyza* spp.**

1236 **(A)** Amplification of *Marf* from cDNA generated from whole body extracts of *S. flava* and *S. pallida*
1237 adults (+RT). As expected, *Marf* does not amplify in templates treated with DNaseI without reverse
1238 transcriptase (– RT), used as a negative control. **(B)** Amplification of *Or67b* genes from *S. pallida* and *S.*
1239 *flava* whole adult cDNA, which reveal *in vivo* transcription of *Or67b* genes in adult *Scaptomyza* (arrow).
1240 Ladder (firsts column) is GeneRuler™ 1 kb plus (ThermoFisher, USA).

1241

1242

1243 **SUPPLEMENTARY FILES**

1244 **Supplementary file 1 Phylogenetic analysis**

1245 Phylogenetic dataset summary, sequence accession numbers, genome sequence coordinates and
1246 phylogenetic model parameters and results.

1247

1248 **Supplementary file 2 Molecular evolution analyses**

1249 Selected parameters and results from branch d_N/d_S tests of all *S. flava* Ors CDS and the expanded *Or67b*
1250 dataset.

1251

1252 **Supplementary file 3 *Or67b* syteny**

1253 The three spreadsheets indicate pGOIs for the three *Or67b* orthologs identified in *S. flava*. For each
1254 sheet, we have the following columns: “Position from GOI in *S. flava*” (e.g. -1 if one gene upstream of
1255 *Or67b*, +2 if two genes downstream of *or67b*); “*S. flava* Annotation ID”; “*D. grimshawi* homolog”
1256 (identified via blastn searches); “*D. grimshawi* homolog scaffold”; “*S. pallida* homolog locations”,
1257 which include scaffold and coordinates; “*D. melanogaster* homolog”, and “*D. melanogaster* homolog
1258 coordinates”. “NA” is written in the cell if homologs were not found after executing blastn, blastx and
1259 tblastx searches.

1260

1261 **Supplementary file 4 PCR primers**

1262 Nucleotides in lower case are either in untranslated sequence (CDS amplification) or are restriction
1263 enzyme cut sites (RE cut site addition). CDS amplification primers were used to amplify full *Or67b*
1264 CDS sequence from cDNA. Primers labeled “RE cut site addition” were used to engineer restriction
1265 enzyme cut-sites via PCR mutagenesis in order to ligate *Or67b* CDS sequences into the pUASTattB
1266 plasmid. All sequences are listed in a 5’ to 3’ orientation.

1267

1268 **Supplementary file 5 Principal component coordinates**

1269

1270 **Supplementary file 6 pGOI sequences**

1271

1272 **Supplementary file 7 list of chemicals**